JOURNAL OF GEOPHYSICAL RESEARCH, VOL. 103, NO. C11, PAGES 25,009–25,027, OCTOBER 15, 1998

# Large structures and temporal change in the Azores Front during the SEMAPHORE experiment

A. Tychensky
Service Hydrographique et Océanographique de la Marine, Centre Militaire d'Océanographie, Toulouse, France

P.-Y. Le Traon and F. Hernandez
Collecte Localisation Satellites, Ramonville St.-Agne, France

D. Jourdan
Service Hydrographique et Océanographique de la Marine, Centre Militaire d'Océanographie, Toulouse, France

**Abstract.** The Structure des Echanges Mer-Atmosphere, Proprietes des Heterogeneites Oceaniques: Recherche Experimentale (SEMAPHORE) mesoscale experiment took place from July to November 1993 in the northern Canary Basin, where the circulation is dominated by the eastward flowing Azores Current (AC). A large data set was acquired from three hydrographic arrays (phases 1, 2, 3), current meter moorings, surface drifters drogued at 150 m, and 2000 m deep RAFOS floats. The analysis confirmed the large-scale observations previously made in this region but also provided new insights into fine-scale dynamics of the AC. The front was observed over the 6-month period. It was narrow (100 km) and mostly surface intensified (velocities reaching 40–50 cm $s^{-1}$). Whereas at the beginning of the experiment (phase 1) the AC was mainly zonal with weak oscillations, large meridional meanders were observed from phase 2 until the end of the experiment. They seem to be related to the arrival of two Mediterranean eddies (Meddies), which interacted with the AC [*Käse and Zenk*, 1996; *Tychensky and Carton*, this issue]. The front had a deep dynamical signature (down to 2000 m), with a 16–18 sverdrup (Sv) volume transport (0–2000 m depth integrated). The southward recirculation branch of the AC near 22°–23°W [*Klein and Siedler*, 1989] corresponds to meridional transport of 5–6 Sv. Then, 4.5 Sv of these waters are recirculating westward (along 31°–32°N). Some interesting new oceanographic results were obtained by examining the RAFOS float trajectories over the abyssal plain. The circulation is similar to that observed at the surface, with mean velocities of about 1–3 cm $s^{-1}$ and eddy kinetic energy <4 $cm^2$ $s^{-2}$. In agreement with the analysis of current meter data this reveals a significant barotropic component in the Azores-Madeira flow field of roughly 3–3.5 cm $s^{-1}$.

## 1. Introduction

The Structure des Echanges Mer-Atmosphere, Proprietes des Heterogeneites Oceaniques: Recherche Experimentale (SEMAPHORE) oceanographic experiment was conducted in the northern Canary Basin, in a 500 × 500 $km^2$ area between the Azores and Madeira Islands from June to November 1993 (Figure 1). It was designed to investigate the air-sea interactions and the three-dimensional mesoscale oceanic circulation in this area [*Eymard et al.*, 1996]. Another objective was to validate and compare TOPEX/POSEIDON (T/P) and ERS-1 altimeter observations with in situ measurements [*Hernandez et al.*, 1995] and to evaluate altimeter and drifter data assimilation techniques [*Dombrowsky and De Mey*, 1992; *Morrow and De Mey*, 1995]. The SEMAPHORE area flow field is dominated by the Azores Front-Current system (AFC), which is an eastern branch of the subtropical North Atlantic gyre [*Klein and Siedler*, 1989]. From the 30 sverdrup (1 Sv = $10^6$ $m^3$ $s^{-1}$) of the Gulf Stream's southern branch, splitting near the Grand Banks, about 10–12 Sv flow southeastward in the upper 800 m, crossing the Mid-Atlantic Ridge (MAR) between 32° and 37°N through the Oceanographers and Hayes fractures zones, to form the Azores Current (AC) [*Käse and Siedler*, 1982; *Siedler et al.*, 1985; *Käse et al.*, 1985; *Gould*, 1985; *Sy*, 1988; *Klein and Siedler*, 1989]. East of the MAR, this strong, narrow current flows at about 34°N within the North Atlantic Central Water, with velocities of up to 40 cm $s^{-1}$. It is associated with the Azores thermohaline Front (AF) characterized by a thermal gradient of about 2°C over 100 km. Then, as part of the gyre, the AC splits into three southward branches, which vary seasonally and interannually and recirculate into the North Equatorial Current [*Stramma and Siedler*, 1988; *Klein and Siedler*, 1989; *Käse and Krauss*, 1996]. From west to east one branch is located just east of the MAR, another lies in the central basin near 23°W, and the third feeds waters of the Canary Current close to the west coast of Africa. The AC is subject to large meandering, with loops of several hundred kilometers, and mesoscale eddies with typical scales of 100–150 km detaching on both sides of the front [*Käse and Siedler*, 1982; *Käse et al.*, 1985; *Siedler et al.*, 1985; *Siedler and Onken*, 1996]. This contributes to fairly large mesoscale variability, which is well evidenced in satellite altimetry [*Le Traon and De Mey*, 1994;



Paper number 98JC00782.
0148-0227/98/98JC-00782$09.00

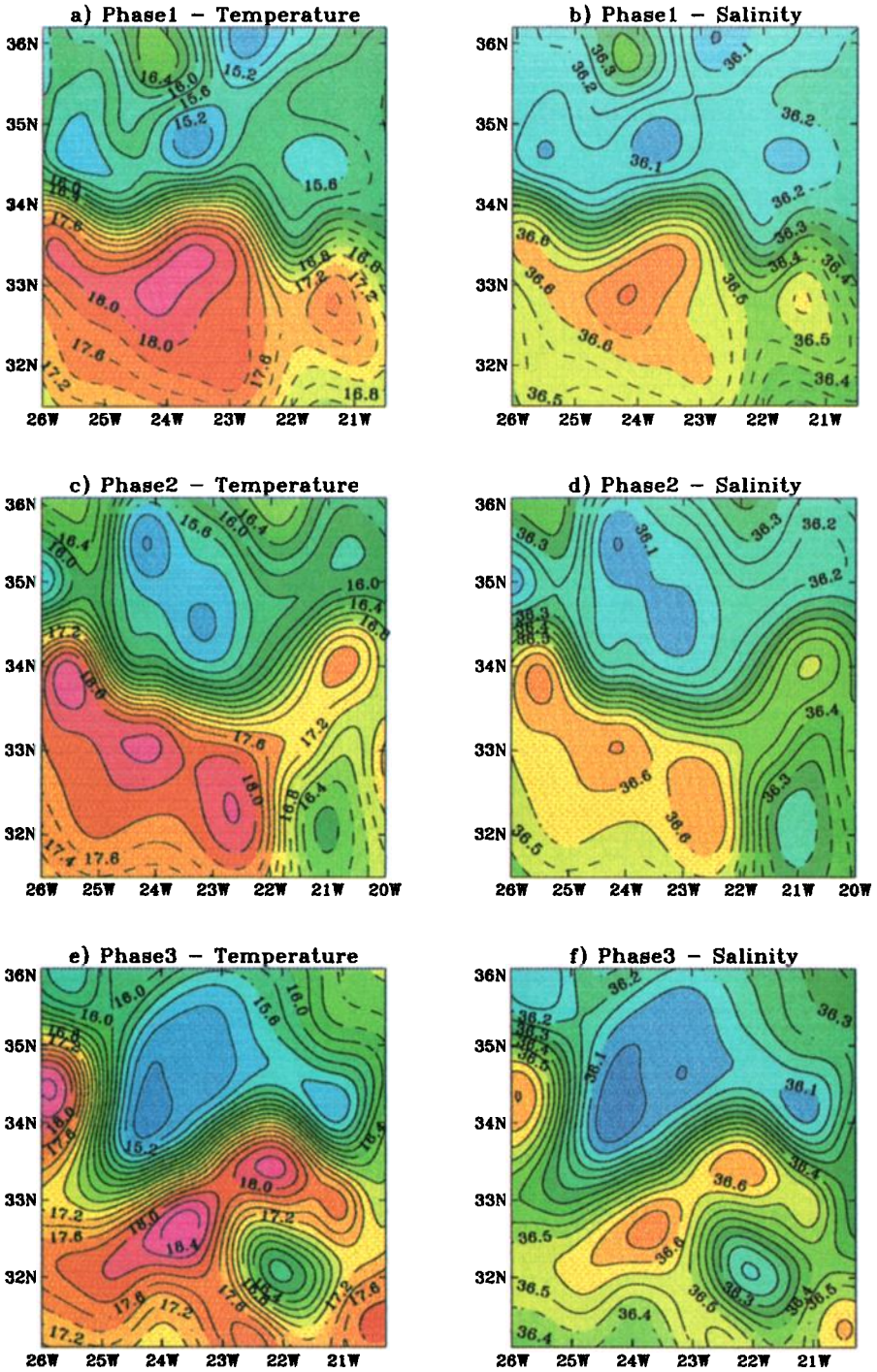


**Plate 1.** Horizontal (Plates 1a, 1c, and 1e) temperature and (Plates 1b, 1d, and 1f) salinity at 150 m depth for phases 1, 2, and 3 computed by objective analysis (OA). Dotted lines indicate areas where estimation errors are >20% of signal variance. Contour interval is 0.2°C and 0.05 practical salinity units (psu) in temperature and salinity, respectively. The thermohaline front associated with the Azores Current is clearly visible during the three consecutive phases. The most noticeable eddy features are (1) a warm, salty eddy first located during phase 1 north of the front on the northern boundary by 35.9°N, 24°W (Plates 1a and 1b); (2) another warm, salty eddy, generated by an anticyclonic meander of the Azores Front, visible during both phases 2 (34°N, 20.5°W) and 3 (33.2°N, 22°W) (Plates 1c–1f); and (3) a cold and fresh eddy south of Meddy 2 during both phases 2 (32°N, 21°W) and 3 (32°N, 22.1°W) (Plates 1c–1f).

*Hernandez et al.*, 1995]. This mesoscale activity is not fully explained and is poorly reproduced by eddy resolving models, even at high resolution [*Spall*, 1990; *Böning and Budich*, 1992; *Beckmann et al.*, 1994; *Käse and Krauss*, 1996]. Three essential mechanisms have however been put forward: baroclinic instability of the AC [*Käse et al.*, 1985; *Kielman and Käse*, 1987; *Käse and Krauss*, 1996], interactions with Rossby waves generated at the eastern boundary [*Le Traon and De Mey*, 1994], and, at

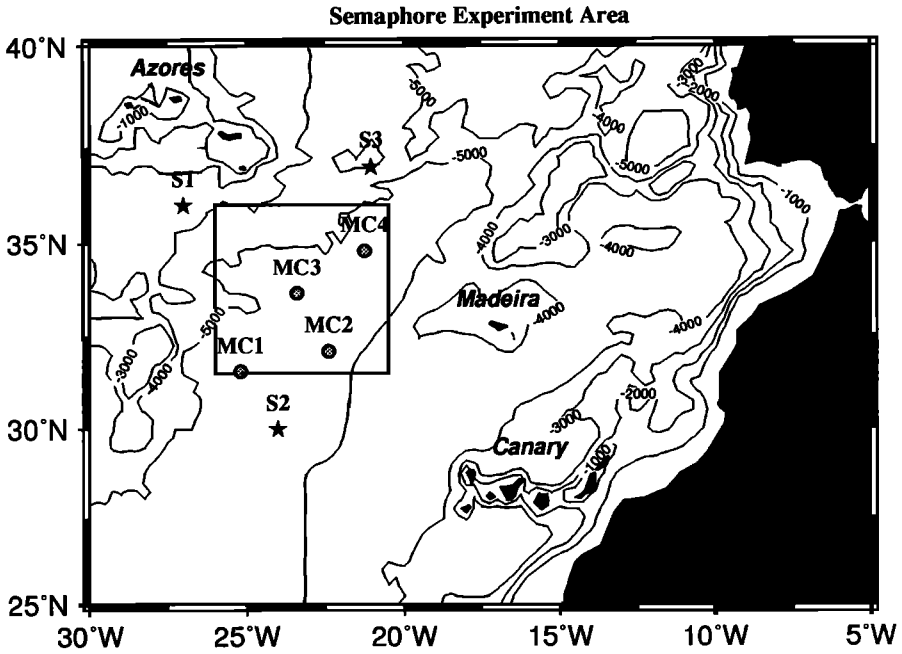


**Figure 1.** The SEMAPHORE experimental area (square box), located in the Azores-Canary Basin. The four current meter moorings are represented by gray circles, and the three acoustic sources are represented by black stars. For details of the moored array, see Table 1. The main topographic features are displayed with the drawing of the 1000- to 5000-m isobaths (every 1000 m).

depths where the Mediterranean water tongue is found (between 800 and 1300 m depth), interactions with eddies of Mediterranean waters (Meddies) [*Käse and Zenk*, 1996; *Tychensky and Carton*, this issue]. The objectives of this paper are to describe and analyze the three-dimensional mesoscale oceanic circulation observed during the SEMAPHORE experiment. We first present the data collected and the processing techniques used. In section 3 we focus on the hydrographic characterization of the area and thermohaline properties of the AF. The next section is dedicated to the velocity fields estimated from hydrography, surface drifter trajectories, and Eulerian current meter measurements. The deep and barotropic circulation are also computed. Finally, we discuss the influence of the Meddies on AC mesoscale instability.

## 2. Data and Processing

The SEMAPHORE in situ measurements was mainly based on hydrography and Lagrangian drifters and floats [*Le Traon and Hernandez*, 1992]. The objective was to precisely observe the Azores Front-Current system over a period longer than the timescale of mesoscale variability in this area [*Le Traon*, 1991; *Le Traon and De Mey*, 1994]. Four current meter moorings were also set up to better infer the vertical structure of the circulation and its barotropic component.

### 2.1. Hydrographic Data

Three hydrographic surveys were performed in July, September, and October–November (phases 1, 2, and 3, respectively; see details in Table 1 and Figures 2b, 2d, and 2f). They were based on both expendable bathythermographs (XBT) and conductivity-temperature-depth (CTD) casts down to 2000 m and performed with a nominal resolution of about 30 nautical miles (55 km). The intermediate survey (phase 2) was performed with XBTs only, with the same spatial resolution, to allow monitoring of the Azores Front and of its eddies between the first and the last survey. Note that the last survey corresponded to the intensive observation period (IOP) of the experiment [*Eymard et al.*, 1996] with five ships involved. The vertical temperature and salinity profiles collected from different ship instruments were compared and did not show any incompatibility. To compute dynamic heights from XBTs (a

**Table 1.** Hydrographic Surveys, Deployment Time for the Surface Drifters and Deep RAFOS Floats, and Vessels Used During the SEMAPHORE Experiment

| Phase | Date | Ship | Hydrography | Surface Drifters | RAFOS Floats |
|---|---|---|---|---|---|
| 1 | July 5–30, 1993 | *Alcyon* | 136 XBT, 49 CTD | 29 | 54 |
| 2 | September 4–13, 1993 | *La Pérouse* | 92 XBT | 6 | 0 |
| 3 | October 12–29 and | *D'Entrecasteaux/* | 155 XBT | 12 | 0 |
| | November 5–11, 1993 | *Ailette/Alcyon* | 43 CTD | | |
| | | *Suroit* | 46 CTD | | |
| | | *Professor Stockmann* | 35 CTD | | |

The RAFOS floats were deployed at 2000 m depth for a duration ranging from 181 days (for the floats programmed for a 6-month mission) to 541 days (for the floats programmed for a 18-month mission).

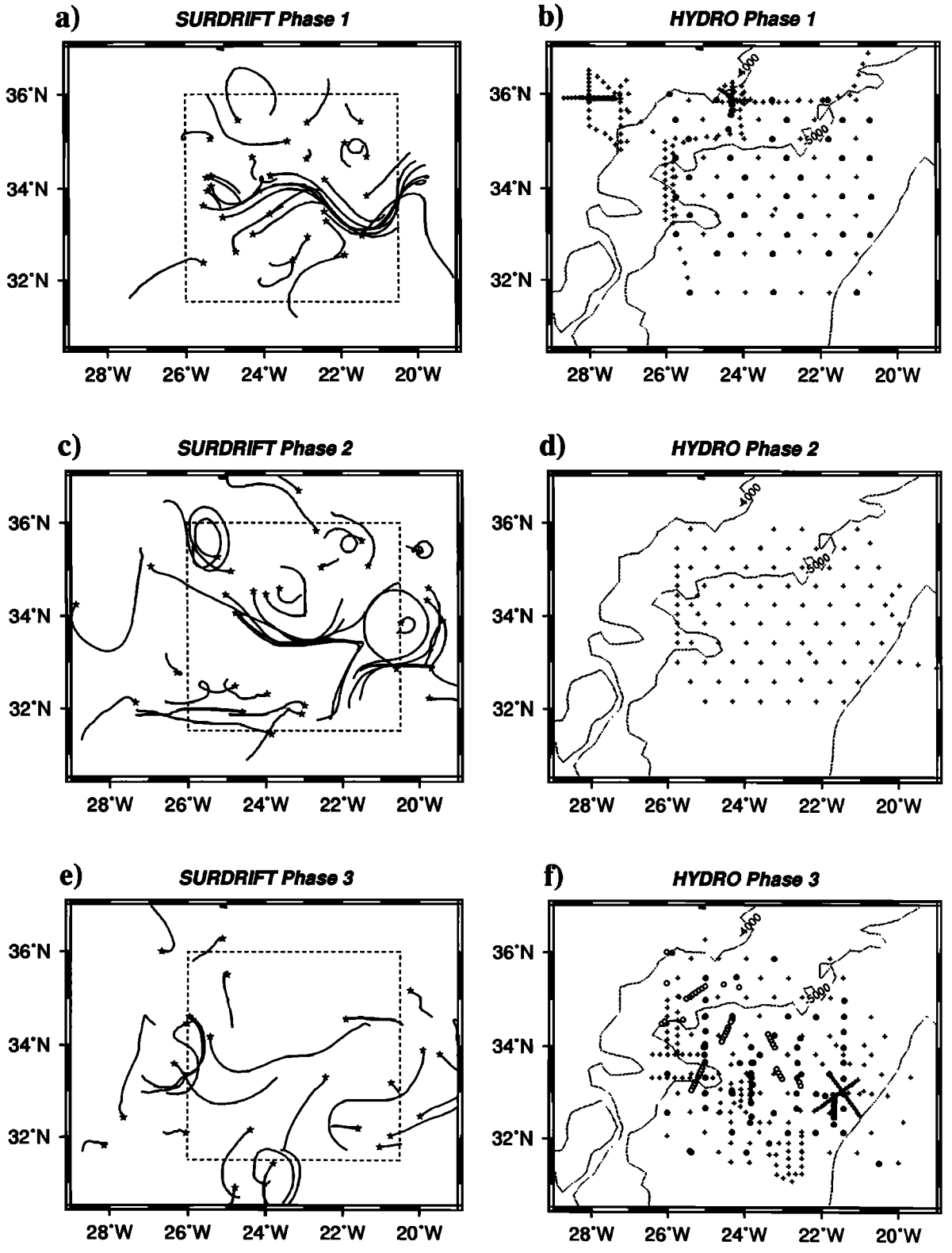


**Figure 2.** Expendable bathythermograph (XBT) (crosses) and conductivity-temperature-depths (CTD) (dots) hydrographic arrays (Figures 2b, 2d, and 2f) for the three phases of the experiment from July to November 1993. Only XBT profiles were acquired during phase 2 (Figure 2d) by the Service Hydrographique et Océanographique de la Marine (SHOM)-French Navy hydrographic ship R/V *La Perouse*. Phase 3 (Figure 2f) was the intensive observation period; CTD profiles came from the SHOM-French Navy Oceanography ship R/V *d'Entrecasteaux*, the Institut Français de Recherche pour l'Exploitation de la Mer (IFREMER) oceanographic ship R/V *Suroît* (open circle), and the Shirshov Institute of Oceanology (Moscow) R/V *Professor Stockmann*. Figures 2a, 2c, and 2e show the trajectories of the surface-type drifters (surdrifts) for each phase. Surdrifts were drogued at 150 m depth. The seeding position of each drifter is marked by a star. The study area is in the center, in dotted lines. The 3000- to 5000-m isobaths are shown as dashed lines.

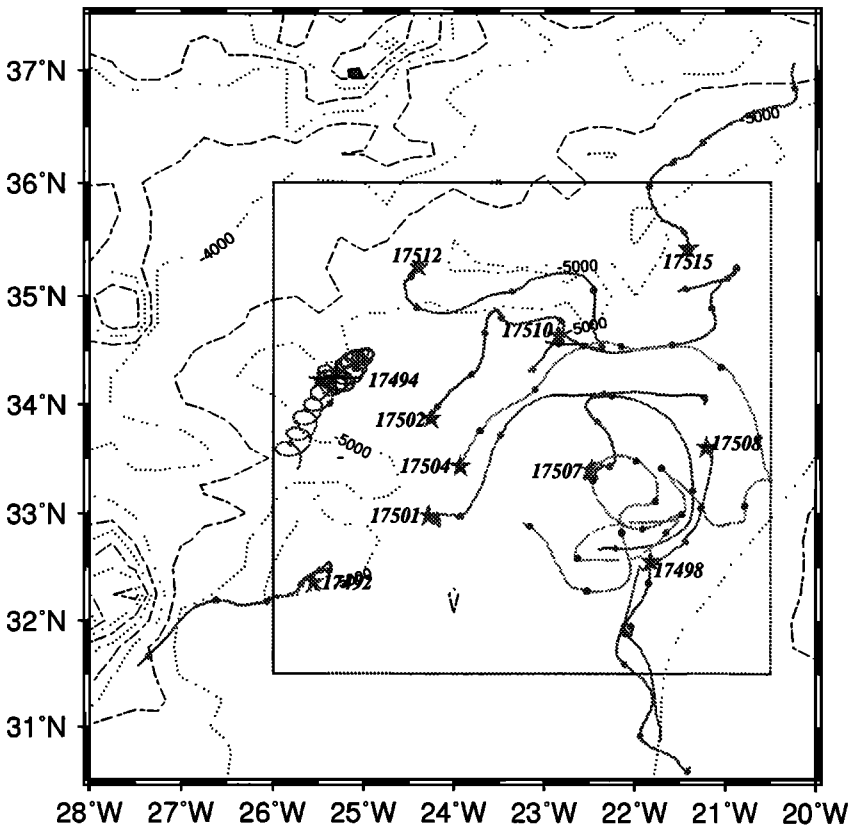


**Figure 3.** Trajectories of 11 deep RAFOS floats deployed at 2000 m depth. The start is indicated by stars and the float number. The points on each trajectory are spaced 1 month apart. The dashed lines are 500-m isobaths, and the study area is represented in the center (dotted line).

reference level of 2000 m was chosen), a salinity profile had to be estimated from the neighboring CTD stations. This technique needs careful implementation in our study area owing to a nonhomogeneous water mass distribution. In particular, Mediterranean Water (MW) and the Meddies, which propagate to the south and southwest and cross the Azores area, cause relatively strong temperature and salinity ($T$-$S$) anomalies, leading to some dispersion in the $T$-$S$ water mass diagram. A dedicated method based on $T$-$S$ linear regressions computed at constant depths in four homogeneous subareas (north and south of the AF, in the AF, and in the meddies; details in work by *Jourdan* [1994]) was used to compute salinity and then density and dynamic heights from XBT data. In the case of phase 2, lacking of CTD measurements, we computed the salinity profiles from the $T$-$S$ linear relations estimated with phase 3 CTDs. The validation criterion of the method was based on dynamic height computation at 150 m (relative to the 2000-m reference level). The resulting accuracy was better than 2 dynamic centimeters (dyn cm) for XBTs. It was estimated to <1 dyn cm for CTDs. All the XBT and CTD profiles were then merged to provide a comprehensive data set and a better description of the mesoscale field. The temperature, salinity, potential density, and dynamic topography at levels spaced every 10 m was then mapped using a space-time objective analysis (OA). OA was performed for the midsurvey date of each of the three hydrographic surveys: July 20, September 7, and October 26. The a priori covariance model of the dynamic topography signal estimated by *Le Traon and De Mey* [1994] in the same area was chosen. The values of the spatial zero crossings were set to 160 and 200 km for the zonal and meridional directions, respectively, and the $e$-folding timescale was set to 20 days. The measurement noise was set to 5 and 20% of the signal variance for CTD and XBT stations, respectively.

### 2.2. Lagrangian Drifters and Floats

Forty-seven surface surface-type drifters (surdrifts) drogued at 150 m and located by the Argos satellite tracking system were deployed to precisely follow the currents below the mixed layer. Figures 2a, 2c, and 2e present the drifter trajectories for each of the three phases. The derived velocities were low-pass filtered with a 3-day cutoff to remove high-frequency oceanic signals such as tidal and inertial currents. The remaining error on the velocity estimations (due to wind slippage, Ekman transport, and unfiltered ageostrophic components) was estimated to $<3$ cm $s^{-1}$ (G. Reverdin and F. Hernandez, unpublished manuscript, 1997). Thanks to a regular deployment of the drifters in the area [*Hernandez et al.*, 1995], dense spatial coverage of the area was obtained for each survey, which permitted us to precisely map dynamic height fields of the mesoscale circulation from drifter velocities using a multivariate analysis [*Le Traon and Hernandez*, 1992]. The velocity covariance functions were derived from dynamic height covariance functions assuming geostrophy.

Fifty-four RAFOS floats, acoustically tracked by three sound sources moored in the Azores-Canary Basin (Figure 1), were seeded at 2000 m during phase 1 to document the deep circulation and to provide an estimate of the velocity field at a deep

**Table 2.** Current Meter

| | Location | | Water Depth, m | Period | | Current Meters | |
|---|---|---|---|---|---|---|---|
| | Latitude, N | Longitude, W | | Range | Duration, days | Number | Depths, m |
| MC1 | 31°42′ | 25°28′ | 5430 | July, 1, 1993 to June 7, 1994 | 342 | 6 | 465, 999, 1475, 2004, 2993, 4082 |
| MC2 | 32°21′ | 22°39′ | 5290 | July 1, 1993, to June 26, 1994 | 361 | 7 | 169, 469, 987, 1501, 2004, 2955, 4076 |
| MC3 | 23°23′ | 33°39′ | 5250 | July 1, 1993 to June 24, 1994 | 359 | 6 | 174, 500, 985, 1540, 2013, 4091 |
| MC4 | 34°48′ | 21°15′ | 5230 | July 1, 1993, to June 23, 1994 | 358 | 7 | 142, 455, 954, 1462, 2014, 2959, 4061 |

The start time and duration refer to daily means of the low-passed filtered series. The minimum duration is 23 days. See Figures 1 and 9.

reference level. Because of technical problems, only 11 RAFOS could be recovered (Figure 3). Trajectories and velocities were computed from the acoustic positioning and low-pass filtered.

### 2.3. Eulerian Current Measurements

Four current meter moorings, each equipped with six current meters regularly spaced vertically (around 150, 500, 1000, 1500, 2000, 3000, and 4000 m), were also deployed for 1 year north and south of the area and in the AC (Figure 1, Table 2). The time series were low-pass filtered with a cutoff frequency below the inertial and tidal frequencies, and daily means were calculated. Note that the moorings were deployed at crossovers of T/P and ERS-1 ground tracks to validate satellite altimetry.

## 3. Water Masses and Hydrographic Features

### 3.1. $\sigma$-$S$ Diagram

The water mass diagram obtained from all CTD measurements is shown on Figure 4. The mixed layer (ML), characterized by high but spatially variable temperature and salinity, progressively deepened from 35 to 80 m between phases 1 and 3, and the overall surface temperatures simultaneously decreased from 22° to 20°C. Below the ML the North Atlantic Central Water (NACW) is characterized by a quasi-linear relation between 150 and 700 m [*Harvey and Arhan*, 1988]. The MW is then found between 700 and 1300 m. This water exhibits noticeable peaks corresponding to the presence of Meddies in the area (see below). This MW tongue overlies the upper North Atlantic Deep Waters (NADW) and strongly influences it by double-diffusion processes, as can be seen by the large variability at about 1300 and 1400 m. Finally, the influence of Labrador Sea Water (LSW) (~3°C, ~34.95 practical salinity units (psu)) can be observed north of the area [*Käse et al.*, 1986; *McCartney and Talley*, 1982; *Paillet et al.*, 1998].

### 3.2. Horizontal Maps and Meridional Sections

Horizontal maps of temperature and salinity at 150 and 1000 m are presented on Plates 1 and 2 for the three phases of the experiment. Plate 3 shows meridional vertical sections of temperature, salinity, and potential density ($\sigma_1$, computed with a 1000-m reference level) through the AF for phases 1 and 3. The AF is conspicuous down to 700–800 m (Plates 3a–3b and 3d–3e), showing a 2.5°C temperature and a 0.4 psu salinity meridional difference over a width of 100 km. It delimits warm and salty waters in the southern part of the front and delimits colder and fresher waters in the northern part. The strongly surface-intensified part of the AF is observed with the vertical slope of both the isotherms and isohalines. In the upper ocean (100–600 m) these isolines define temperature and salinity layers of constant thickness, which sink to about 145 m when crossing the front southward. In other terms, vertical gradients of both temperature and salinity stay rather identical on both sides of the front. Between 700 and 1200–1300 m the front signature decreases considerably due to the presence of the MW tongue and mesoscale activity associated with the Meddies. The analyzed 1000-m maps (Plate 2) clearly reveal two distinct MW lenses, which can be observed at the close vicinity of the AF during the three consecutive surveys (for a complete description of these features, see *Tychensky and Carton* [this issue]. These two Meddies are centered around 1000 m, and

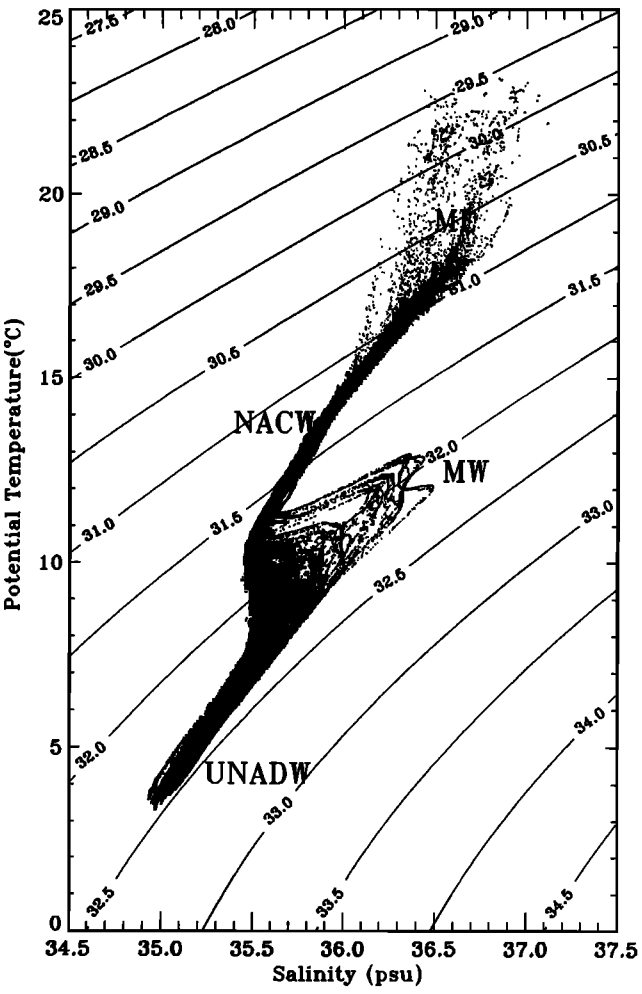


**Figure 4.** Potential $T$-$S$ diagram including the main water masses (see text), computed from all the CTD observations acquired during phases 1 and 3 between the surface and the depth of 2000–2500 m. Also shown are isopycnal lines referenced to 1000 m depth (units are $\sigma_1$ − 1000 kg m$^{-3}$).

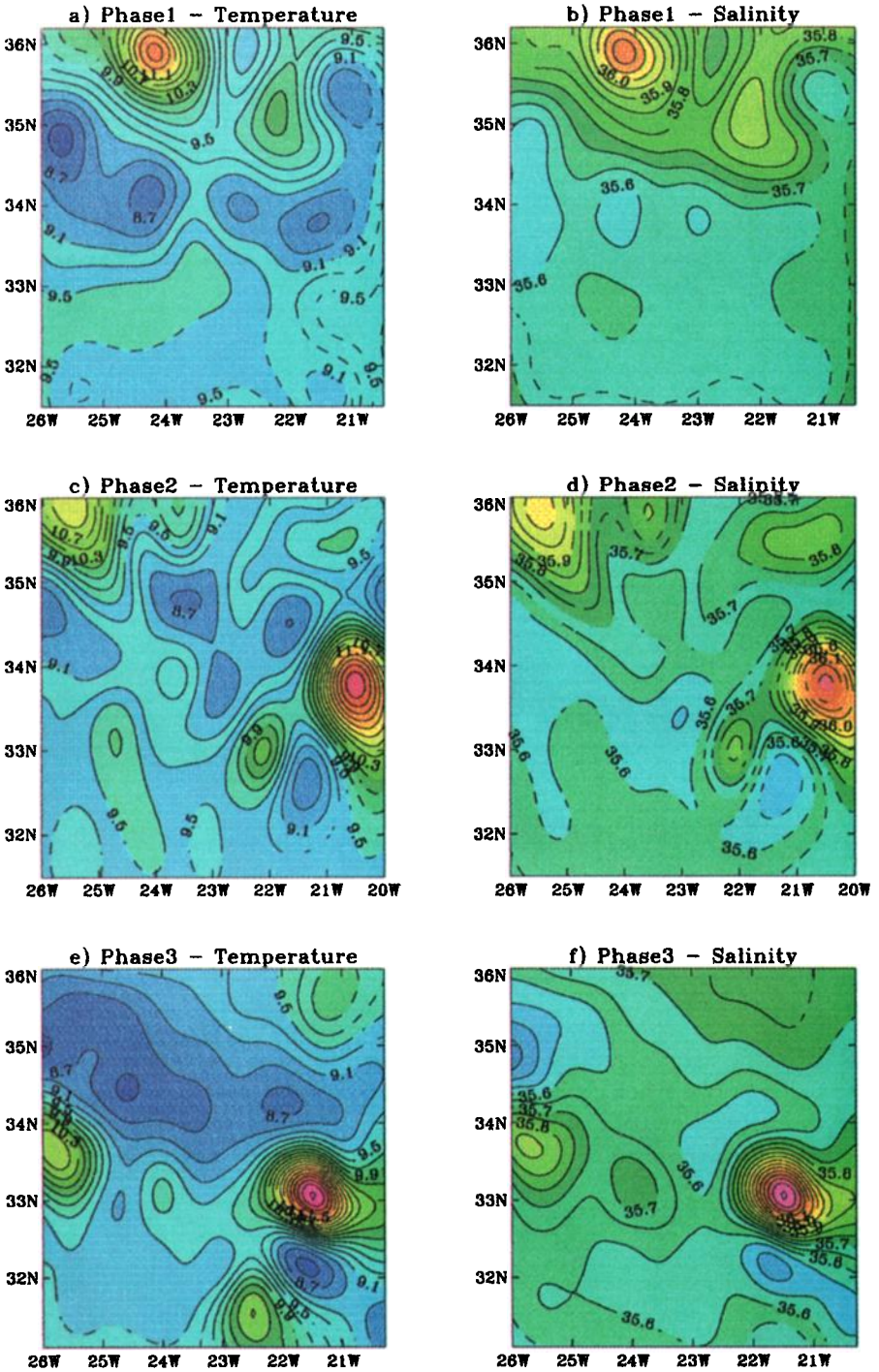


**Plate 2.** Maps of (Plates 2a, 2c, and 2e) temperature and (Plates 2b, 2d, and 2f) salinity at 1000 m depth (see Plate 1 for details). The dominant signal is associated with Meddy 1 (see Plates 2a and 2b, 35.9°N, 24.2°W; Plates 2c and 2d, 35.9°N, 25.5°W; and Plates 2e and 2f, 33.7°N, 25.9°W) and meddy 2 (see Plates 2c and 2d, 33.8°N, 20.5°W and Plates 2e and 2f, 33.1°N, 21.5°W). Also observed is the deep signature of the cold, fresh surface eddy located south of Meddy 2 during both phases 2 (32.5°N, 21.5°W) and 3 (32.1°N, 21.5°W).

their diameters are between 60 and 100 km. Meddy 1 (called Cérès), first located on the northern boundary (36°N, 24°W) during phase 1, is observable again in the northwestern corner during phase 2 (36°N, 25.5°W) and then on the western boundary (33.8°N, 25.7°W), embedded in the AF during phase 3. During both phases 1 and 2 this Meddy is associated with a warm, salty surface anomaly (Plate 1). The second Meddy (called Encelade) appears at the eastern boundary during phase 2 (33.8°N, 20.5°W), propagating southwestward between phases 2 and 3. This meddy is associated during these phases with a cold, fresh eddy located on its southern flank (32.2°N, 21°W during phase 2 and 32°N, 22°W during phase 3) (see Plates 2c–2f). Although surface intensified (its maximum thermohaline anomalies are found at 150 m), this cyclonic feature has a vertically extended signature visible down to 1400 m. This feature intensifies in a strong dipole-like structure with Meddy

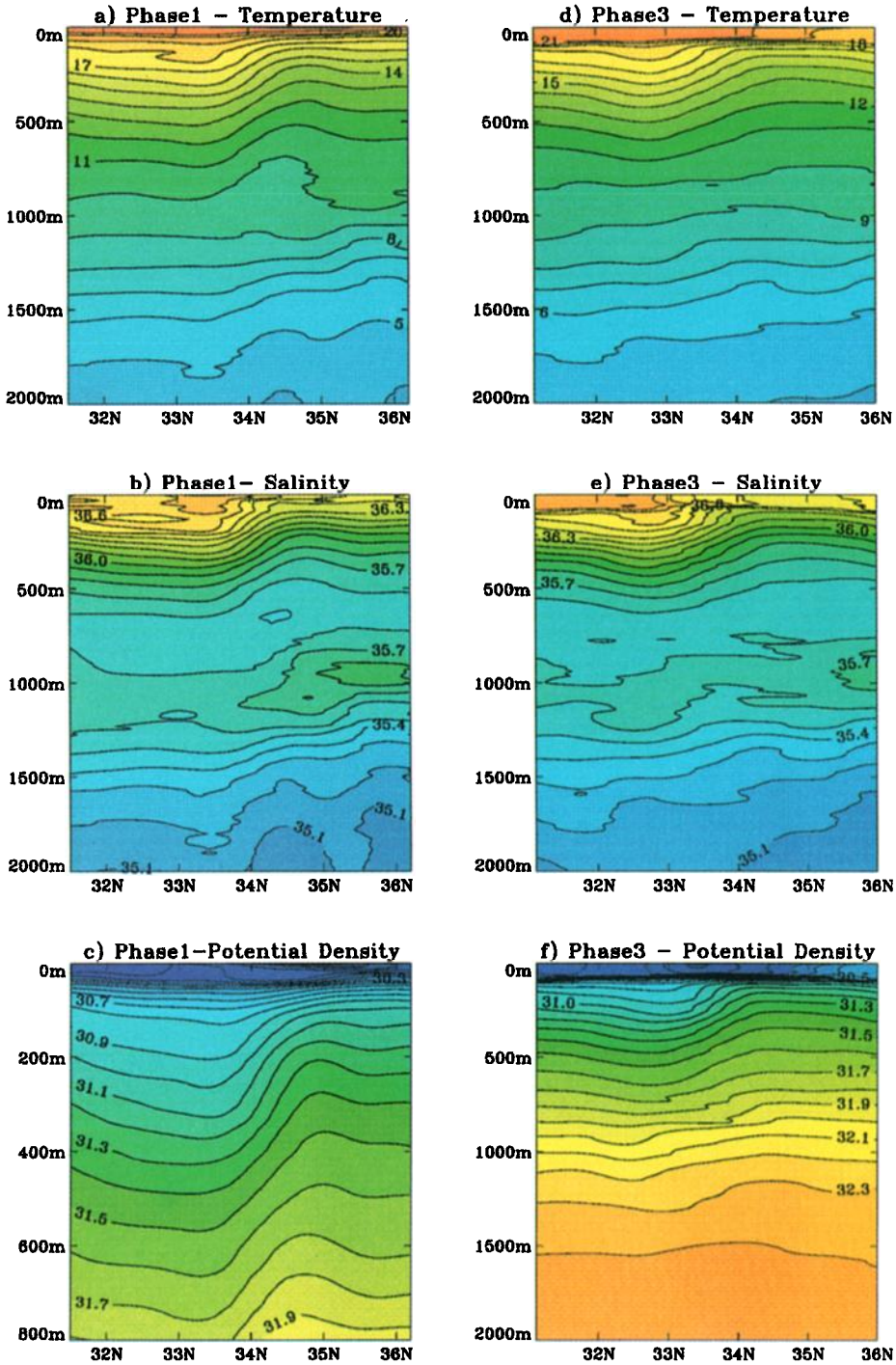


**Plate 3.** Vertical meridional sections at 23.2°W. Distribution of (Plates 3a and 3d) temperature, (Plates 3b and 3e) salinity, and (Plates 3c and 3f) potential density across the Azores Front for phases 1 and 3, mapped by OA. Increments for isotherms and isohalines are 1°C and 0.1 psu, respectively. The density distribution is referred to 1000 m depth. The indicated labels correspond to $\sigma_1$ − 1000 kg m$^{-3}$, and contour intervals correspond to 0.1 kg m$^{-3}$. The density section in Plate 3f shows a strong, extended dynamical signal related to the Azores Front, intensified in the 0–1000-m layer and weaker below. Plate 3c shows a blowup of the upper 800 m depth of the dynamical signal associated with the Azores Current.

2 during phase 3. A water mass analysis (not shown) indicates that this cold eddy is formed with waters similar to waters located north of the AF.

The MW tongue is characterized on the area by a fairly homogeneous layer associated with low vertical gradients and average salinities of about 35.58 psu. The relative salinity maxima appear at 1000 m and reach about 35.82 psu during phase 1. They are found north of the front (Plates 2b and 3b), in agreement with the *Sy* [1988] MW circulation scheme. However, these maxima are no longer observed during phase 3 (Plates 2f and 3e), probably because of the development of large meanders and mixing effects of MW on both sides of the

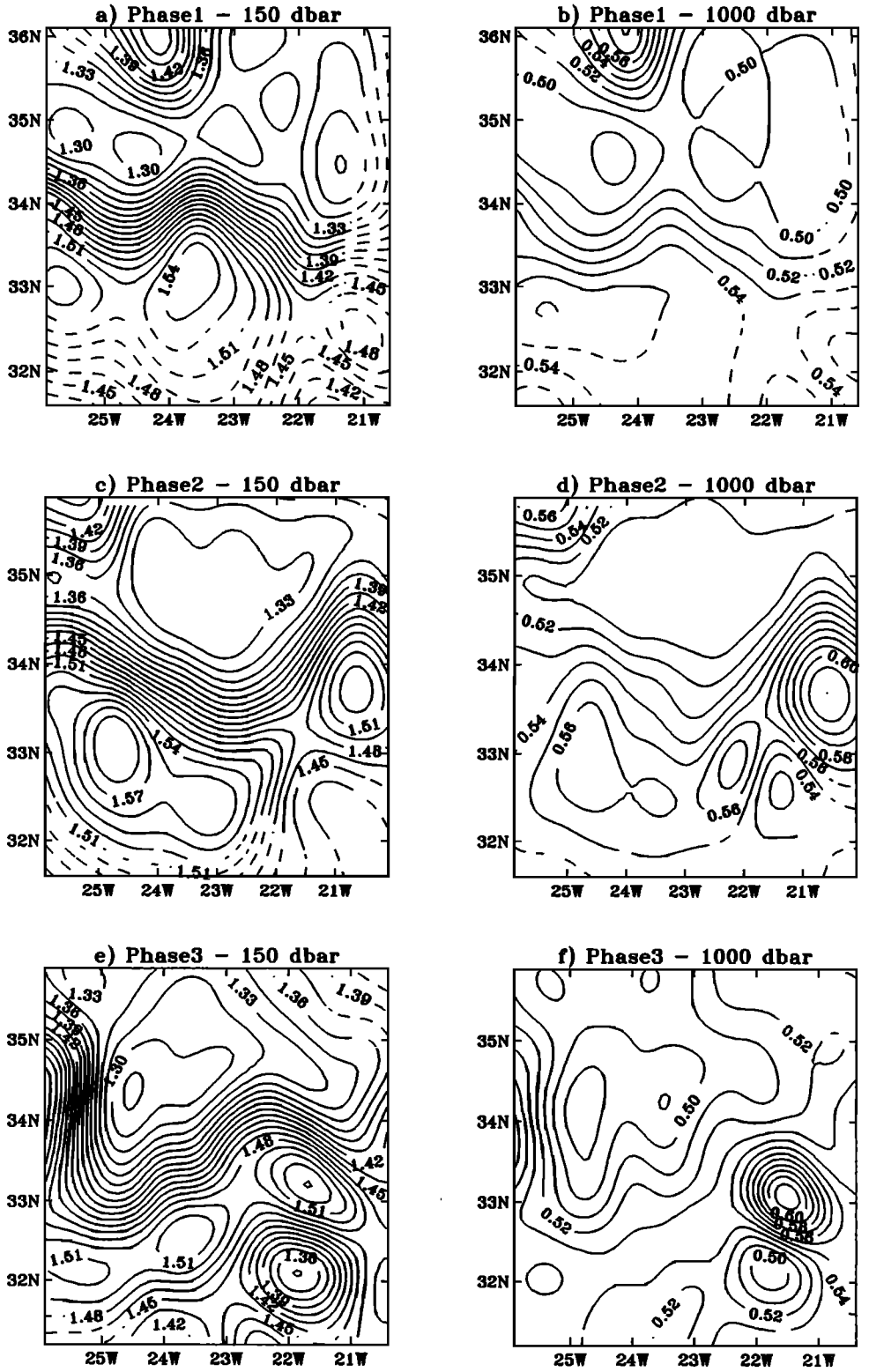


**Figure 5.** Objectively analyzed dynamic topography maps (relative to 2000 dbar) given in dynamical meters (dyn. m) at 150 and 1000 dbar for (a, b) phase 1, (c, d) phase 2, and (e, f) phase 3. Contours with dashed lines correspond to estimation errors >20% of the signal variance.

Azores Front. The meridional thermohaline gradient associated with the AF in the surface waters appears again at a depth of 1500 m and below, as shown by meridional slopping of both isotherms and isohalines over the whole section (Plate 3). At these depths this may come from a contribution of modified Labrador Sea Waters (LSW), which propagate southward in the eastern North Atlantic basin between 1500 and 2500 m depth [*McCartney and Talley*, 1982; *Paillet et al.*, this issue], and

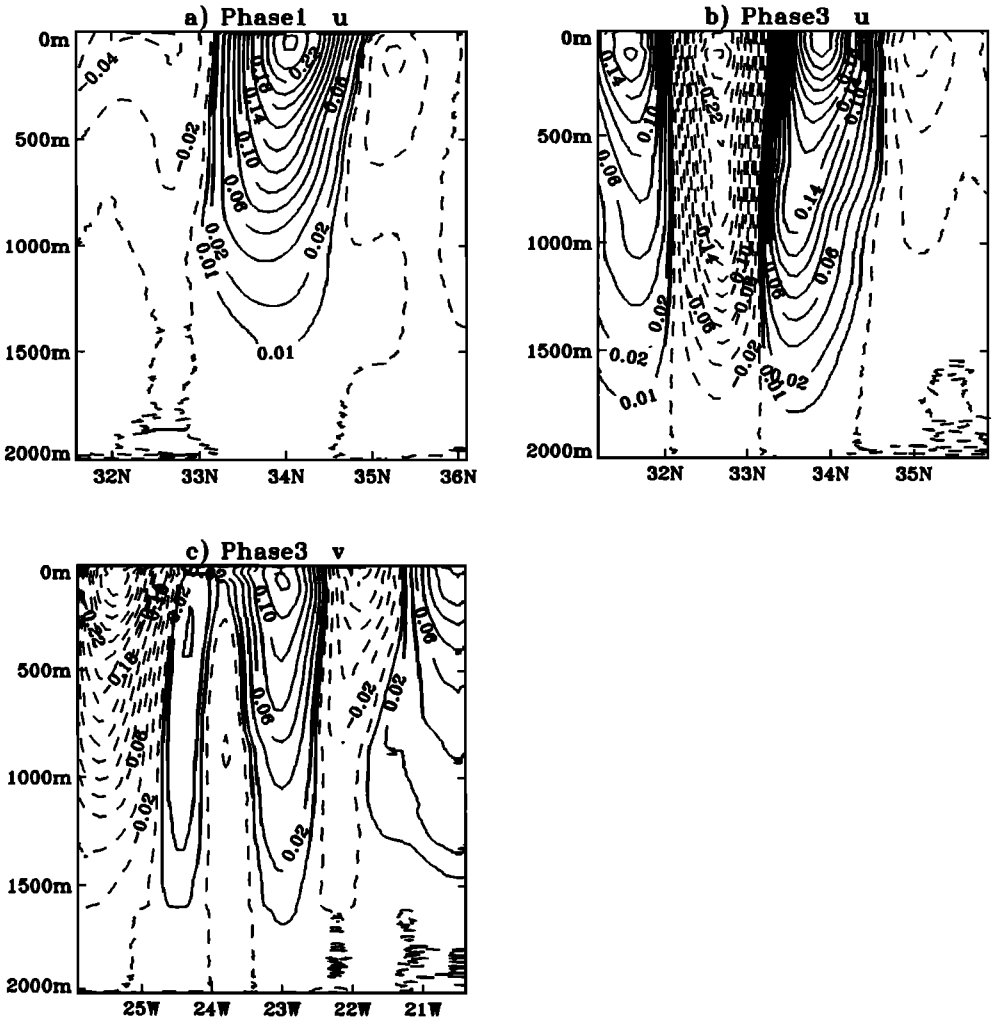


**Figure 6.** Vertical sections of geostrophic velocity components in m $s^{-1}$. Meridional sections of the zonal component are shown (a) through the AC during phase 1 at 23.2°W and (b) through the dipole (Meddy cyclone) during phase 3 at 21.8°W. (c) The meridional branch of the meander west of the area is shown in the zonal section of the meridional component at 34.2°N during phase 3. Sign convention is positive for eastward and northward components (solid lines); negative values are represented by the dashed lines.

may have extension boundaries in the northern part of our experimental area. On the vertical sections of potential density (Plates 3c and 3f) we observe a coherent and well-extended dynamic signal, marked by slopping of isopycnal surfaces observable over the whole water column. Note that the temperature and salinity anomalies associated with the presence of the MW tongue almost compensate each other, resulting in no specific signature of this water mass in density. The vertical distribution of the density field thus reveals the deep density structure of the AC, associated with a dynamical signature down to 2000 m depth. The presence of the MW seems to mark only a vertical thermohaline discontinuity in the 2000-m penetration depth of the AF.

## 4. Circulation

We now present the oceanic circulation near the AC as computed geostrophically from hydrography and as measured by the Lagrangian floats (surdrifts and RAFOS) and the current meter moorings.

### 4.1. Geostrophic Circulation and Transport

Geostrophic currents were computed from the hydrographic measurements with a reference level at 2000 m depth. This level was chosen since it is the deepest level common to CTDs and XBTs. Moreover, barotropic structures such as the cold cyclonic patch observed south of Meddy 2 and Meddies, which are associated with a deep dynamical signature, did not reveal any intermediate level of minimum circulation. This was also confirmed by the current meter moorings.

As will be seen later, RAFOS floats at 2000 m depth and current meter moorings show that the velocities at this reference level were nonzero but could reach 1–3 cm $s^{-1}$ (which is significant). Figure 5 shows the analyzed dynamic height maps at 150 and 1000 m depth for phases 1–3 of SEMAPHORE, while Figure 6 presents the corresponding meridional and zonal vertical sections of components $u$, $v$ through the AC. During the experiment the AC exhibits a maximum dynamic height gradient of 20–24 dyn cm over a 100–120-km width near the surface. This gradient decreases to 4–5 dyn cm at 1000 m

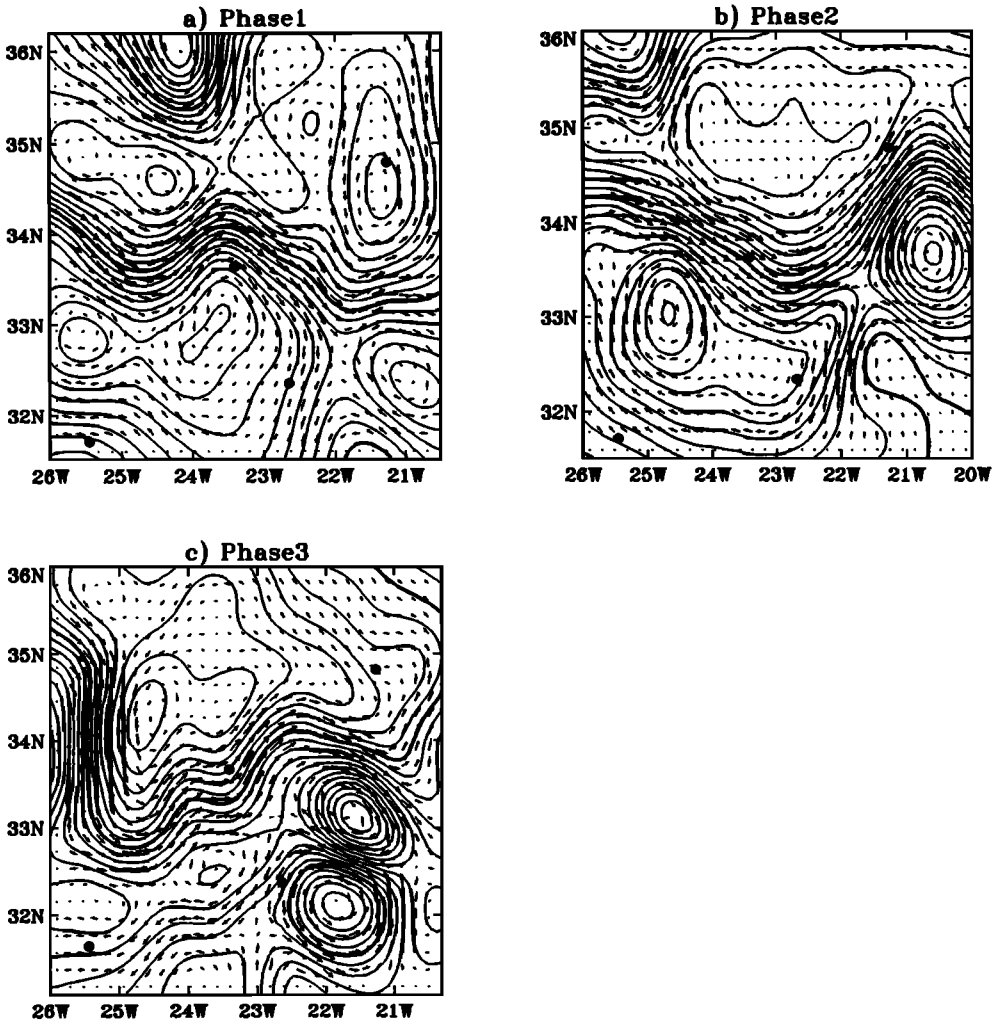


**Figure 7.** Geostrophic volume transport streamlines in sverdrups (Sv) integrated from 2000 m depth to the sea surface, for (a) phase 1, (b) phase 2, and (c) phase 3. Contour interval is 1.5 Sv (1 Sv = $10^6$ $m^3$ $s^{-1}$). The geostrophic currents at 150 m referenced to 2000 m are overlaid (thin arrows). Dots indicate mooring positions (see also Figure 1).

depth. The associated zonal geostrophic velocities in the jet thus reach 24–26 cm $s^{-1}$ at 150 m depth and about 4 cm $s^{-1}$ at 1000 m depth. Because of our choice of reference level the AC is only visible here over the first 1500–1700-m depth of the fluid column (Figures 6a–6c).

At 1000 m depth (Figures 5b, 5d, and 5f) the dominant signal is related to the presence of the Meddies (a 10 dyn cm gradient over a 35-km radius for Meddy 1 during phase 1 and a 12 dyn cm gradient over 45 km from the central axis for Meddy 2 during phase 3) and to the cold cyclone moving south of Meddy 2. During phase 2 this cyclone presents a weak signature on the 150- and 1000-m-depth topographic dynamic fields but strongly intensifies during phase 3 (a 10.5 and 4.5 dyn cm gradient at 150 and 1000 m depth, respectively). The three consecutive 1000-m-depth maps show that Meddy 2 is entering the area, propagating southwestward and interacting with the AC during phase 2. The AC path is then deflected to the north and forms an anticyclonic loop, which circles around the fluid column advected with the Meddy propagation. This generates a surface anticyclonic anomaly, which aligns vertically with the Meddy. Consequently, it forms a strong anticyclonic fluid column associated with maximum velocities ranging from 30 cm $s^{-1}$ at 150 m depth to 25 cm $s^{-1}$ at 1000 m depth. Although the cold cyclone south of the Meddy 2 is surface intensified, it is also present over the same fluid column as that advected by Meddy 2 and forms a strong dipole-like feature with both this Meddy and the surface anticyclonic meander. The vertical section at 21.8°W (Figure 6b) shows that the dynamical signal associated with this dipole structure is coherent down to 1800 m depth, below the Meddy level. Thus Meddy 2 seems to have a driving effect over the vertical and generates a barotropic fluid column. Velocity records of current meter MC2 (not shown) made on the mean axis of this dipole corroborate this mechanism and actually suggest an even deeper extension down to 4000 m depth, where maximum velocities of 5 cm $s^{-1}$ were measured. In the western part of the area the AC axis tends to shift from west-east to north-south during phase 3. Such meandering of the current may be due to the interaction with Meddy 1. The surprising trajectory of this Meddy during the experiment seems to corroborate this assumption. It first propagates westward until late September, also driving its overlying anticyclonic companion (seen also with the surface drifter trajectories on Figures 2a and 2c). Then, while interacting with and crossing the AC, the Meddy seems to be de-

flected south (this is confirmed by the RAFOS float trajectories [see *Richardson and Tychensky*, this issue]. Maximum velocities in the AC were observed in the strongest meanders. Meridional geostrophic velocities thus reached up to 35 cm $s^{-1}$ at 150 m depth in the meander west of the area and reached 28–30 cm $s^{-1}$ in the anticyclonic meander surrounding Meddy 2. At least, one of the southward recirculation branches of the AC is clearly seen near 23°W during the first 3 months of the experiment, in agreement with the climatology of the region [*Klein and Siedler*, 1989]. It feeds a westward return flow (Figures 5a and 5c), where velocities at 150 m depth are about 8–10 cm $s^{-1}$. This return flow is strongly modified by the dipole during phase 3 (Figure 5e).

We then computed volume transport on the area from a vertical integration of the geostrophic velocities from 2000 m depth up to the surface. A 16–18-Sv transport was estimated for the AC during phases 1–3 (Figure 7). But we can observe some lateral recirculations on both sides of the AC system for each of the three periods. Taking these recirculations into account (contribution of the eddies associated with the AC) yields higher values for volume transport, of about 20–22 Sv. Our transport values are significantly higher than the historical values of 12 Sv in the upper 1500-m depth given by *Gould* [1985] or the 12–13 Sv estimated by *Sy* [1988] and *Krauss et al.* [1990]. However, estimating the transport over the whole width of the area reduces the zonal transport to ~6.5 Sv at the western boundary (because of the opposite contribution of the westward return circulation south of the AC and of the flow field associated with Meddy 1) and to ~8.5 Sv at the eastern boundary. Finally, the reference level is not of major importance for the calculation of the geostrophic transport as mentioned by *Stramma* [1984]. In fact, most of the transport is given by the first 1000-m-depth contribution (90% of the total). However, a 2 cm $s^{-1}$ mean velocity at 2000 m depth would increase the AC transport by about 4 Sv, i.e., from 16 to 20 Sv. Note that 4–5 Sv recirculate southward in the meridional branch. The water transport associated with each of the Meddies is 10–12 Sv.

### 4.2. Absolute Velocity Measurements

**4.2.1. Contribution of drifters to the description of the surface circulation at 150 m depth.** The velocities deduced from drifters are, generally, stronger than that estimated by hydrography. The difference is mainly explained by the spatial resolution of the hydrographic arrays (55 km), which smooths out the gradients, and, to a less extent, by the barotropic component not measured by the hydrography. Figure 8 displays dynamic height fields at 150 m depth mapped by multivariate analysis [*Le Traon and Hernandez*, 1992] from the surface drifter trajectories. The overall picture described by the drifters is consistent with the hydrography, but surdrifts provide a better representation of the frontal structures and the mesoscale eddy features. In particular, they clearly show the intensification of the AC meanders. The estimated gradients were steeper, associated with velocities ranging from 40 to 50 cm $s^{-1}$ in the western part of the front and in the meanders and ranging from 20 to 30 cm $s^{-1}$ in its eastern part. Surdrifts were also trapped in several of the most energetic surface eddies (Figure 2). For instance, the anticyclonic eddy above Meddy 1 propagated westward with a speed of 2 km $d^{-1}$. The velocities in this eddy were stronger than the one deduced from hydrography and reached 30 cm $s^{-1}$ at a 20-km radius. During phases 2 and 3 several drifters followed the fluid column generated by

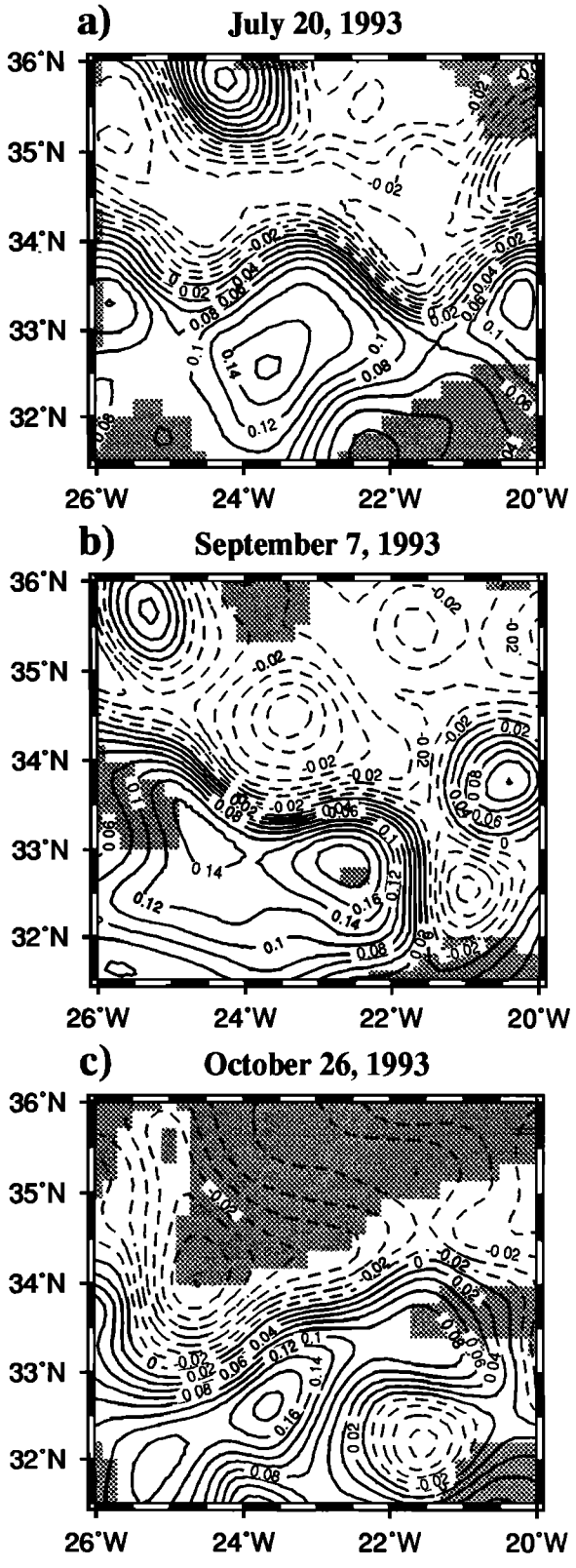


**Figure 8.** Dynamic height fields at 150 m depth, relative to 2000 m depth in dyn. m (a spatial mean is removed to better represent positive and negative features). The maps are computed for (a) phase 1, (b) phase 2, and (c) phase 3 from the surdrift trajectories by multivariate analysis. Dashed areas correspond to estimation error above 40% of the signal variance.

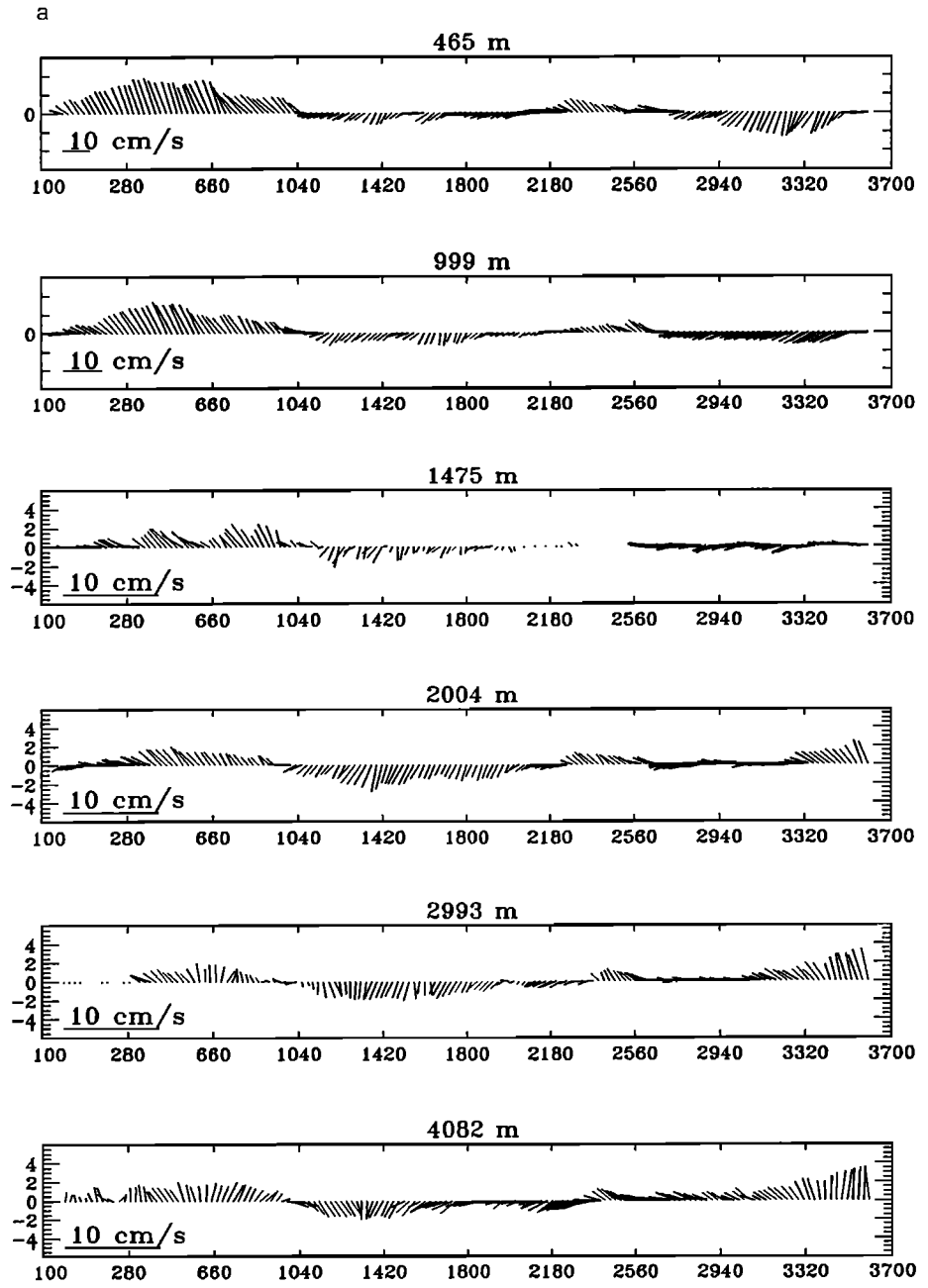


**Figure 9.** Vector time series of daily means for current meter moorings (a) MC1, (b) MC2, (c) MC3, and (d) MC4 at the indicated depth levels for the 6-month period of the SEMAPHORE experiment. Mooring locations are given in Figures 1 and 7. The records start on July 7 (time 0000 LT of the $x$ axis) and stop on November 30 (time 3700 LT of the $x$ axis). The $x$ axis units are hours. In the upper 1000-m depth, velocities are plotted between $-15$ and 15 cm $s^{-1}$ (5 cm $s^{-1}$ ticks) for MC1 (Figure 9a) and MC4 (Figure 9d) and between $-32$ and 32 cm $s^{-1}$ for MC2 (Figure 9b) and MC3 (Figure 9c). Velocities of the deeper current meters are all plotted between $-6$ and 6 cm $s^{-1}$.

the vertical alignment of the surface anticyclonic meander with Meddy 2. They propagated to the west-southwest at about 3.3 km $d^{-1}$ and azimuthal velocities at 150 m depth reached 40 cm $s^{-1}$ at an 80-km distance from the column central axis. Note that the cold cyclone associated with Meddy 2 is better described during phase 2 on the surdrift map (Figures 8b and 8c) than on the hydrographic data set (Figures 5c and 5e). It appears, since this period, as a 100-km-radius coherent feature, with rotating speeds, given by the drifters trapped in it, of about 20 cm $s^{-1}$. This cyclone is then observed to propagate at the same speed and direction as the fluid column advected by Meddy 2. Finally, the drifters indicate that the southward recirculation branch of the AC at 22°–23°W is slightly more intense (maximum velocities reach 12–14 cm $s^{-1}$). This may be due to a barotropic component in the circulation branch; the surdrifts show during phase 2 (Figure 2c) that part of this southward flow turns to the right at 32°N. It forms a westward return current, located between 30° and 33°N, with velocities of about 10–12 cm $s^{-1}$. Drifters were advected by this return current until September, and some of them were then ab-

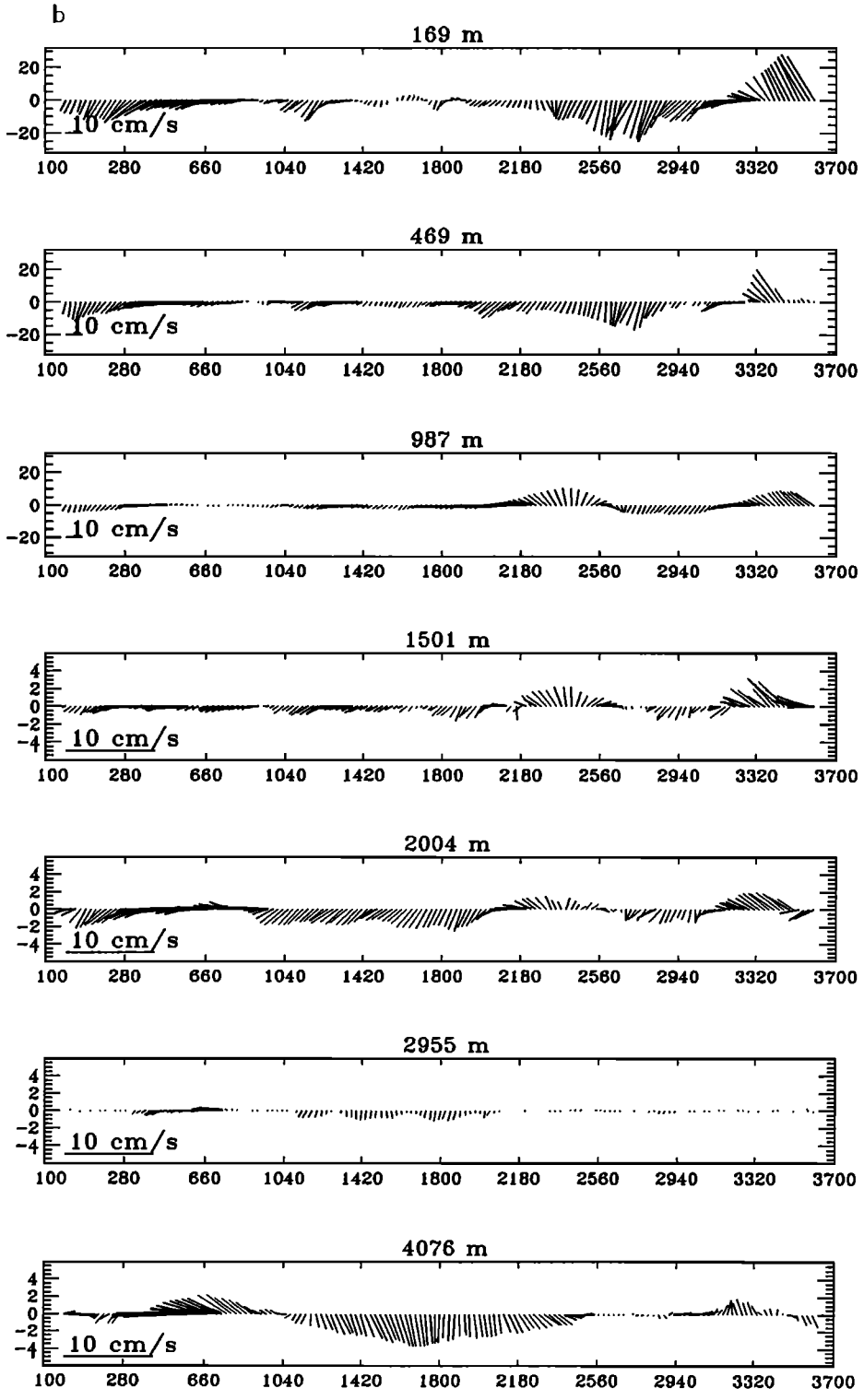


**Figure 9.** (continued)

sorbed in October and November by the water column advected by Meddy 1, which is located at that time on the western boundary of the experimental area near 34°N, 26°W (see Figures 2e and 8c).

**4.2.2. Vertical structure of the currents as measured by current meter moorings.** The analysis of the current meter data set is limited here to a 6-month period corresponding to the SEMAPHORE experiment. Figures 9a–9d show the vector time series of the four moorings at their various recording depths. MC3 was lying mostly on the AC axis (Figures 1 and 7). The mooring indicates a mean zonal eastward circulation associated with velocities of 22 cm $s^{-1}$ at 174 m depth (Table 3) and maximum velocities up to 32 cm $s^{-1}$. This agrees well with earlier figures given by *Müller and Siedler* [1992] (a mean value of 20 cm $s^{-1}$ at 200 m depth). Maxima of velocities decrease to 4 cm $s^{-1}$ below 2000 m depth. In the top 500-m depth the

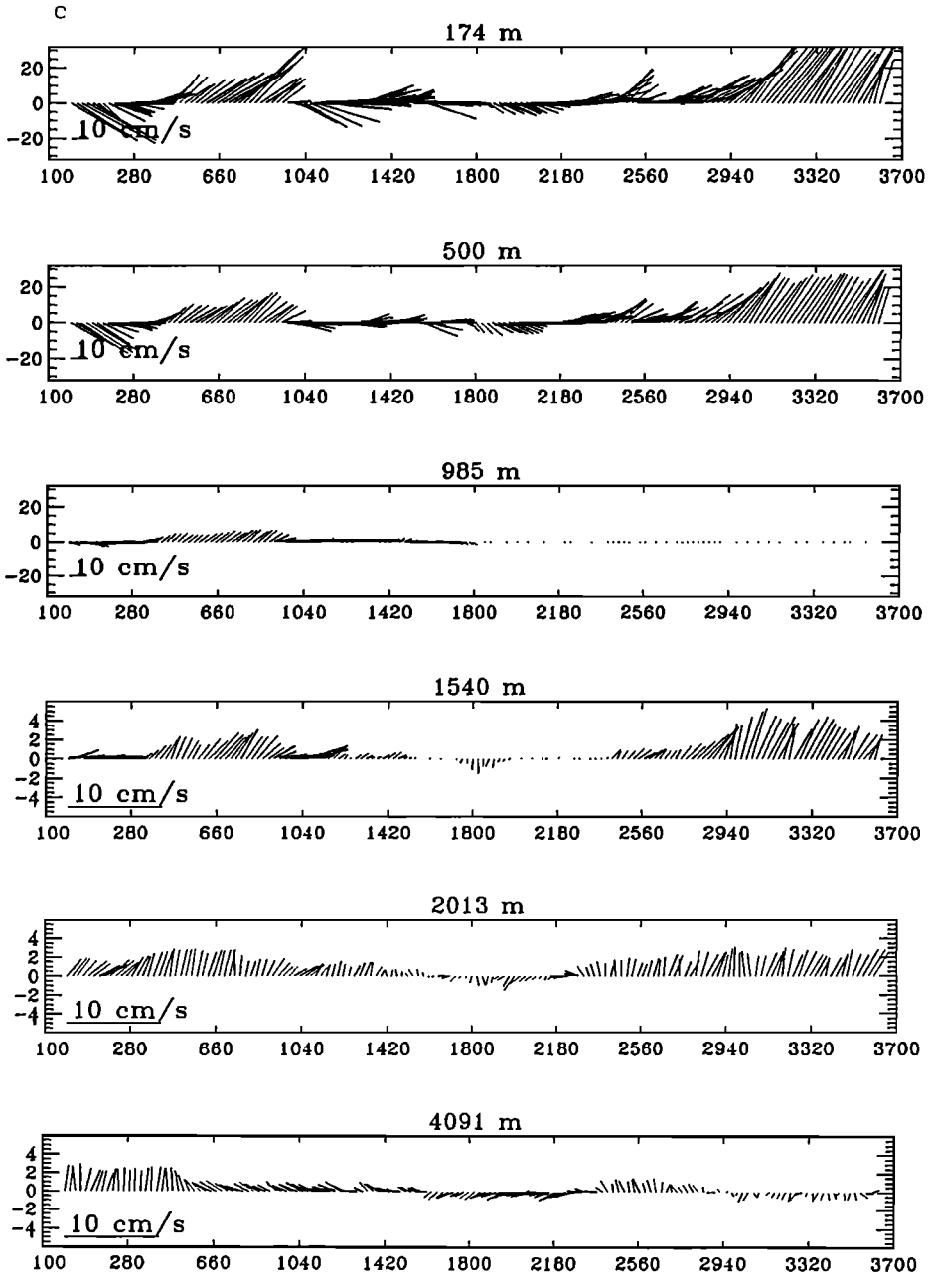


**Figure 9.** (continued)

current fluctuates between the southeast and northeast directions with timescales of about 75 days (Figure 9c). This mesoscale signal is associated with rapid change in the frontal structure (displacement of the AC meanders) [*Siedler et al.*, 1985]. The good vertical consistency in this mesoscale signal suggests a significant barotropic component. However, below 1540 m depth we observe some vertical phase reversal, which is indicative of baroclinic flows (see the modal decomposition below). MC2, south of the front, was mainly embedded in the southern recirculation branch of the AC (Figures 1 and 7). The current is vertically coherent during the first half of the period and is generally oriented south-southwest. In the second half of the record a reversal of the current related to rather strong anticyclonic velocities (8–12 cm $s^{-1}$) and temperature anomalies (0.7°C at 987 m depth and 0.5°C at 1501 m depth) can be observed between the 987- and 2004-m-depth levels. This small event suggests the passage of a small warm anticyclonic eddy through the mooring site between phases 2 and 3, which may originate in the fragmentation of Meddy 2 while crossing the AC. Moorings MC1 and MC4 indicate much weaker mean velocities of 4–8 cm $s^{-1}$ (maxima reaching up to 8–10 cm $s^{-1}$) in the surface levels. The currents were generally oriented to the west in MC1 (north, then south, see Figure 9a). This mooring thus confirms the presence of the westward return flow south of the AC, as extension of the AC southward recirculation branch. In the 2000–4000-m-depth layer the mean currents decrease to 1.3–1.5 cm $s^{-1}$, with local maxima <4 cm $s^{-1}$. Velocities recorded at MC4 are mostly oriented to the north-northeast. The mean northward recirculation of the AC, observed northeast of the area with MC4 during this 6-month

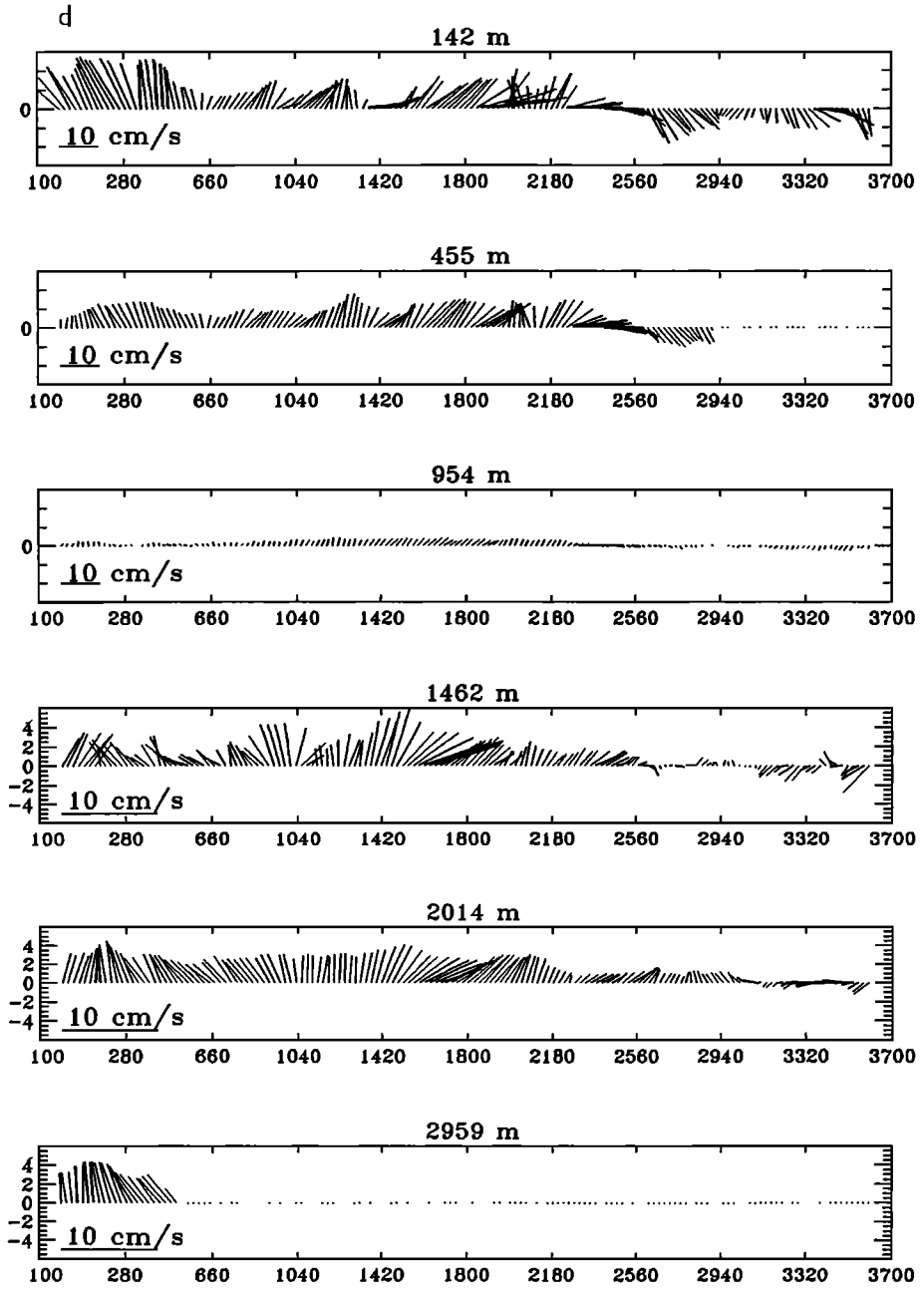


**Figure 9.** (continued)

period, may be related to a northward meander constrained by the arrival of Meddy 2 at the northeastern boundary of the experimental area. Note also that the currents show good vertical amplitude and phase consistency at the MC1 and MC4 moorings. This means that the barotropic flow is strong at these two sites.

Statistics for the variability have been computed from the moorings for the zonal and meridional components of the velocity selected over the 6-month period (Table 3). The regional distribution indicates higher variability, mostly concentrated near the AC (moorings MC2 and MC3), reaching values up to 130 $cm^2\ s^{-2}$ at 170 m depth, while in the northeastern part of the area this variability stays below 30 $cm^2\ s^{-2}$. A stronger contribution to the eddy kinetic energy (EKE) is found in the meridional component. The meridional velocity variance is larger by a factor of 1.5–3 than the zonal variance above the thermocline and still stays greater until the 2000- and 4000-m-depth levels in the AC. There is thus a strong anisotropy between zonal and meridional fluctuations of the circulation field. Notice that the average velocities show the main zonal direction of the AC, whereas the larger meridional fluctuations show that the AC is subject to significant spatial variations and meanders. Moreover, this anisotropy characterizes the preferential north-south fluctuations of the AC meanders. This result corroborates the anisotropy shown by satellite altimetry [*Le Traon and De Mey*, 1994].

**4.2.3. Vertical mode decomposition.** The decomposition into dynamical modes enables us to separate the barotropic and baroclinic components of the current. Only the barotropic and the first two baroclinic modes were used in this study and

**Table 3.** Statistical Analysis of the 6-Month Current Meter Data

| Depths, m | $\bar{u}(z)$, cm s$^{-1}$ | $\bar{v}(z)$, cm s$^{-1}$ | $\bar{U}(z)$, cm s$^{-1}$ | $\overline{u'^2}(z)$, cm$^2$ s$^{-2}$ | $\overline{v'^2}(z)$, cm$^2$ s$^{-2}$ | $\frac{1}{2}\overline{u'^2 + v'^2}(z)$, cm$^2$ s$^{-2}$ | $\overline{u'v'}(z)$, cm$^2$ s$^{-2}$ |
|---|---|---|---|---|---|---|---|
| | | | *MC1* | | | | |
| 465 | −4.7 | 0.7 | 6.1 | 1.5 | 16.5 | 9.0 | −0.8 |
| 999 | −3.4 | 0.4 | 4.5 | 1.8 | 9.9 | 5.8 | 0.1 |
| 1475 | −1.0 | 0.1 | 1.3 | 0.6 | 0.7 | 0.6 | −0.1 |
| 2004 | −1.4 | −0.02 | 1.8 | 0.3 | 1.3 | 0.8 | −0.2 |
| 2860 | −0.7 | −0.1 | 1.4 | 0.4 | 1.3 | 0.8 | −0.1 |
| 4082 | −0.8 | 0.3 | 1.8 | 1.3 | 1.7 | 1.5 | 0.2 |
| Average | 1.8 | 0.3 | 2.6 | 0.9 | 4.6 | 2.7 | −0.1 |
| | | | *MC2* | | | | |
| 170 | −7.2 | −4.9 | 12.0 | 25.0 | 92.6 | 58.8 | −4.3 |
| 469 | −5.1 | −3.7 | 7.6 | 10.0 | 25.8 | 17.9 | −3.0 |
| 987 | −3.3 | −0.3 | 5.2 | 9.4 | 15.3 | 12.4 | −3.4 |
| 1501 | −1.0 | −0.1 | 1.4 | 0.8 | 0.8 | 0.8 | −0.2 |
| 2005 | −1.5 | −0.6 | 2.1 | 0.7 | 1.2 | 1.0 | −0.1 |
| 4077 | −0.3 | −0.7 | 2.0 | 2.7 | 2.3 | 2.5 | −1.2 |
| Average | −1.9 | −1.1 | 3.4 | 4.8 | 11.2 | 8.0 | −1.4 |
| | | | *MC3* | | | | |
| 174 | 22.0 | 8.6 | 27.0 | 58.3 | 206.2 | 132.6 | 7.7 |
| 501 | 16.4 | 7.2 | 20.5 | 17.5 | 123.6 | 70.6 | 3.2 |
| 985 | 6.0 | 1.7 | 6.6 | 5.0 | 6.2 | 5.6 | 2.0 |
| 1540 | 1.1 | 1.2 | 1.9 | 0.9 | 2.0 | 1.5 | 0.8 |
| 2014 | 0.4 | 1.4 | 1.8 | 0.5 | 1.2 | 0.9 | 0.4 |
| 4091 | −0.7 | 0.5 | 1.4 | 0.5 | 1.1 | 0.8 | 0.2 |
| Average | 3.6 | 2.1 | 5.5 | 6.5 | 2.6 | 16.6 | 1.3 |
| | | | *MC4* | | | | |
| 158 | 3.1 | 3.0 | 8.1 | 23.9 | 35.0 | 29.4 | 10.7 |
| 455 | 2.8 | 3.6 | 6.4 | 11.8 | 11.9 | 11.8 | −2.8 |
| 955 | 0.4 | 0.6 | 1.3 | 0.7 | 0.8 | 0.7 | 0.5 |
| 1462 | 0.4 | 1.5 | 2.4 | 3.6 | 2.3 | 3.0 | 1.0 |
| 2014 | 0.2 | 1.9 | 2.6 | 3.1 | 1.6 | 2.3 | 0.4 |
| 2959 | −1.3 | 3.2 | 3.6 | 0.7 | 1.2 | 0.9 | −0.02 |
| Average | −1.0 | 2.6 | 3.6 | 3.8 | 4.4 | 4.1 | −0.6 |

Averages and variances of the velocity's meridional and zonal components are calculated, and also, the eddy kinetic energies and Reynolds stresses are calculated for the four moorings and at each recording level. For each mooring a vertically integrated average is estimated for all these quantities.

were a good approximation of the vertical flow structure. The vertical profile of Brunt-Väisälä frequency required for the dynamical mode computation was obtained from mean temperature and salinity profiles from the whole CTD set. Note that an extra calculation of the Brunt-Väisälä frequency using data in the vicinity of each current meter did not change the modal vertical decomposition. The first baroclinic mode has a zero crossing near 1400 m depth, while the second mode exhibits maximum values at 800 m depth. Table 4 summarizes the various contributions of these modes at each depth of the current meter moorings.

The current is mostly barotropic in MC1 and MC4, as was shown above on Figures 9a and 9d. This gives some hints about the possible large-scale barotropic component of the circulation, outside the path of the AC. However, the baroclinicity is considerably increased in the AC (MC3) and its vicinity (MC2). We clearly see the importance of the second baroclinic mode between 987 and 1501 m depth, related to the passage of the small baroclinic feature of MW. Vertically integrated, the first baroclinic mode is predominant in MC2 and MC3 and represents 44.5 and 71% of the signal, respectively. While the first baroclinic mode is strongly dominant in the top 500-m depth, the barotropic mode is particularly significant in the deep layers and contributes to >50% of the signal on all sites below the 1400–1500-m-depth levels. This yields a mean barotropic component on the order of 3–3.5 cm s$^{-1}$ in there.

**4.2.4. Deep circulation as deduced from RAFOS float trajectories.** The deep circulation in the Canary Basin is poorly known. Early information suggests eastward flows in the abyssal plain lower than a few cm s$^{-1}$ [*Müller and Siedler*, 1992]. Though few trajectories were available, our 11 RAFOS floats provided valuable data sets to further analyze the deep circulation. In 6 months the floats typically moved up to 300–400 km, corresponding to mean velocities of the flow field of 1.5–2.5 cm s$^{-1}$ and to EKE <3 cm$^2$ s$^{-2}$ (Figure 3). These Lagrangian estimates are in good agreement with mean Eulerian velocities computed at 2000 m depth from the four moorings (velocities between 1.8 and 2.6 cm s$^{-1}$). The 2000-m-depth oceanic circulation surprisingly includes noticeable eddy activity and a significant influence of the bathymetry, particularly in the southward and northward flows observed to the northeast and southeast of the area (see RAFOS 17512, 17515, 17502, 17508, and 17498, which follow the 5000-m-depth isobath). Over the abyssal plain the RAFOS float trajectories describe a large anticyclonic loop associated with velocity maxima of up to 8 cm s$^{-1}$. On the one hand, this anticyclonic deep circulation seems to follow the boundaries of the abyssal plain, as indicated by the 4000- and 5000-m-depth isobaths. On the other hand, this loop also seems to reproduce the circulation pattern observed in the upper layers, which is consistent with a significant barotropic component of the flow field estimated in the area. In agreement with the analysis of the previous sections

the RAFOS float trajectories may show the 2000-m-depth deep dynamical signature of the AC, or at least, their drifts agree with a theoretical loop of the subtropical gyre waters at the ocean basin eastern border. Finally, we note the surprising trajectory of RAFOS 17494 trapped in an anticyclonic feature, which first propagates northeastward at about 0.5 km $d^{-1}$ and then southeastward at about 1.5 km $d^{-1}$. The azimuthal velocities vary between 5 and 12 cm $s^{-1}$, and the orbital period varies between 6 and 8 days. A CTD survey performed initially in the near vicinity, when the RAFOS was launched, indicates cold, fresh waters. This feature could correspond to a Labrador Sea eddy [*Elliot and Sanford*, 1986]. In a recent work, *Paillet et al.* [1998] suggest that anticyclonic eddies may be generated by baroclinic instability of the thermohaline front formed by the confluence of LSW and deep MW.

## 5. Discussion and Conclusion

The large set of SEMAPHORE in situ measurements has provided new insights into the dynamics and variability of the Azores Front-Current system. The Azores Front, together with surface eddy activity on both sides, was visible around 34°N. These eddies were about 100–150 km in diameter. The surface warm and salty eddy located above Meddy 1, whose origin is not explained, is interesting. This feature may come from waters located south of the front and would have been generated by instability of the AC and vorticity shedding. However, we lack observational data, and a water mass analysis does not yield any conclusions. Recent work on the dynamical instability of the Azores Front-Current system [*Alves*, 1996], based on observations and numerical simulations, evidences the presence of strong anticyclonic eddies generated north of the frontal area. Note that these turbulent mesoscale features are able, in turn, through rectification processes, to generate a westward countercurrent on the northern flank of the Azores Current jet [e.g., *Cromwell et al.*, 1996]. Altimeter data, combined with the dense coverage of in situ measurements, should allow the estimation of the absolute circulation in the area, thus providing successive synoptic views to assess the origin of these return flows.

Though its dynamical signature extends deeply over the first 2000-m-depth of the fluid column, the AC is strongly intensified in its upper part above the thermocline. Geostrophic volume transport integrated over the 2000 m was estimated at 16–18 Sv, with a larger contribution of the first 1000-m depth. This transport is higher than previous estimates [e.g., *Gould*, 1985; *Sy*, 1988]. This may be due to the high-density sampling of the hydrographic data across the AC, which provides steeper gradients and stronger velocities. Taking into account lateral recirculation cells observed on both sides of the front increases these transport estimates to about 4 Sv. One of the three southward recirculation branches of the AC, which is associated with a significant southward flow (4–5 Sv), was observed near 22°–23°W in agreement with *Klein and Siedler*'s [1989] climatological estimates. During SEMAPHORE we observed a significant enhancement of the meander amplitudes on the AC over a few months. Maximum horizontal velocities were found in the strongest meanders. This rapid, abrupt change in the AC meanders seems, first, to have been significantly constrained by the proximity of two Meddies and, second, to have strongly modified the structure of the southward recirculation. From phase 2 the AC develops large-amplitude meanders, sometimes associated with intense meridional extensions, as, for instance, the particularly marked one (250 km) generated in the western part of the area by the crossing of the AC by Meddy 1. The surprising trajectory followed by Meddy 1 and the presence of a cold, deep cyclone propagating in a strong baroclinic dipole with Meddy 2 allow us to suggest Meddy-AC interaction processes. *Tychensky and Carton* [this issue] provide quantitative analysis of all these structures and a numerical experiment that supports their interpretation as an interaction Meddy-AC [see also *Käse and Krauss*, 1996]. The cyclonic eddy may have been generated by occlusion and subsequent shedding of a cyclonic meander of the AC (under baroclinic instability triggered by the meddies). This explains its water characteristic similarities with the colder and fresher waters north of the front.

Surface drifters revealed a narrower, more intense jet. Peak velocities of 45 or even 50 cm $s^{-1}$ were recorded in the AC by both the surface drifters and moorings MC2 and MC3 (maxima of up to 47 cm $s^{-1}$ at 174 m depth), compared with maximum velocities of 25–30 cm $s^{-1}$ measured by hydrography. Outside the Azores Current, in particular to the southeast and northeast of the area, current meter moorings MC1 and MC4 revealed a region of lower activity. Below 2000 m depth the flow field seems to be more homogeneous in the study area, with average velocities ranging from 2 to 2.5 cm $s^{-1}$, in agreement with information supplied by the RAFOS data set. The vertical mode decomposition showed the stronger baroclinicity

**Table 4.** Decomposition of the Current Meter Velocity Vectors Into the Barotropic and First Two Baroclinic Modes

| Depths, m | Barotropic | First Baroclinic | Second Baroclinic | Cumulative, % |
|---|---|---|---|---|
| | | *MC1* | | |
| 465 | 21.1 | 77.3 | 1.2 | 99.6 |
| 999 | 56.5 | 14.4 | 21.0 | 91.9 |
| 1475 | 74.3 | 1.1 | 11.2 | 86.6 |
| 2004 | 77.3 | 10.4 | 1.4 | 89.1 |
| 2860 | 72.2 | 22. | 1.4 | 95.6 |
| 4082 | 68.8 | 24.5 | 3.4 | 96.7 |
| Average, % | 51.8 | 39.7 | 4.4 | 95.9 |
| | | *MC2* | | |
| 170 | 9.8 | 74.4 | 9.6 | 93.8 |
| 469 | 14.8 | 71.7 | 0.5 | 87 |
| 987 | 29.6 | 18.0 | 40.9 | 88.5 |
| 1501 | 50.3 | 2.0 | 26.7 | 79.0 |
| 2005 | 62.6 | 22.1 | 1.5 | 86.2 |
| 4077 | 54.0 | 33.3 | 7.9 | 95.2 |
| Average, % | 34.1 | 44.5 | 11.1 | 89.7 |
| | | *MC3* | | |
| 174 | 4.6 | 89.8 | 4.2 | 98.6 |
| 501 | 7.3 | 88.5 | 1.0 | 96.8 |
| 985 | 33.8 | 45.2 | 18.3 | 97.3 |
| 1540 | 59.7 | 1.6 | 30.4 | 91.7 |
| 2014 | 48.5 | 45.5 | 1.3 | 95.3 |
| 4091 | 35.6 | 57.5 | 5.2 | 98.3 |
| Average, % | 21. | 71.3 | 4.8 | 97.1 |
| | | *MC4* | | |
| 158 | 13.5 | 66.4 | 8.7 | 88.6 |
| 455 | 21.1 | 65.6 | 0.7 | 87.4 |
| 955 | 36.1 | 19.7 | 21.3 | 77.1 |
| 1462 | 58.9 | 1.1 | 25.6 | 85.6 |
| 2014 | 62.8 | 5.3 | 8.7 | 76.8 |
| 2959 | 84.5 | 6.9 | 7.4 | 99.0 |
| Average, % | 59.3 | 23.7 | 8.9 | 91.9 |

For each of the four current meter moorings the relative energy of each mode at each level and the vertical integration are given.

of the currents in and near the AC, whereas the barotropic component seems to dominate generally everywhere else. The latter was estimated to be about 3–3.5 cm $s^{-1}$ in the study area. Finally, the deep RAFOS floats revealed a deep anticyclonic circulation at 2000 m depth. They also revealed a Labrador Sea Water eddy, thought to be generated by baroclinic instability of the thermohaline front between deep MW and LSW [*Paillet et al.*, 1998].

The SEMAPHORE in situ data set will be extremely useful in the future. The different data (hydrography, drifters, floats, and Eulerian current measurements) will soon be combined via an inverse model to make better estimations of the three-dimensional circulation during the three arrays. The data set will then be used to test the ability of the model to predict changes in the Azores Front and will be used for a quantitative analysis of its dynamics.

**Acknowledgments.** The authors express their gratitude to Yves Camus, Bruno Le Squère, Pascal Canceill, and the CMO group for help in data processing. Special thanks go to E. Plakhin and to L. Prieur for providing us with their CTD data. Thanks are also due to Xavier Carton and Jerome Paillet for their essential help and useful comments on the manuscript. Discussions with Phil Richardson, Gille Reverdin, Pierre De Mey, Eric Dombrowsky, Laurence Eymard, and Rosemary Morrow were greatly appreciated. This work is a contribution to the SEMAPHORE mesoscale dynamics research program. Financial support for this work was provided by the Service Hydrographique et Océanographique de la Marine (France).

## References

Alves, M., Instability dynamics of a subtropical jet: The Azores Front-Current system case, Ph.D. thesis, Univ. de Bretagne Occidentale, Brest, France.

Beckmann, A., C. W. Böning, C. Köberle, and J. Willebrand, Effects of increased horizontal resolution in a simulation of the North Atlantic Ocean, *J. Phys. Oceanogr.*, *24*, 326–344, 1994.

Böning, C. W., and R. G. Budich, Eddy dynamics in a primitive equation model: Sensitivity to horizontal resolution and friction, *J. Phys. Oceanogr.*, *22*, 361–381, 1992.

Cromwell, D., P. G. Challenor, A. L. New, and R. D. Pingree, Persistent westward flow in the Azores Current as seen from altimetry and hydrography, *J. Geophys. Res.*, *101*, 11,923–11,933, 1996.

Dombrowsky, E., and P. De Mey, Continuous assimilation in an open domain of the Northeast Atlantic, 1, Methodology and application to AthenA-88, *J. Geophys. Res.*, *97*, 9719–9731, 1992.

Elliott, B., and T. B. Sanford, The subthermocline lens D1, I, Description of water properties and velocity profiles, *J. Phys. Oceanogr.*, *16*, 532–548, 1986.

Eymard, L., et al., Study of the air-sea interactions at the mesoscale: The SEMAPHORE experiment, *Ann. Geophys.*, *14*, 986–1015, 1996.

Gould, W. J., Physical oceanography of the Azores Front, *Prog. Oceanogr.*, *14*, 167–190, 1985.

Harvey, J., and M. Arhan, The water masses of the central North Atlantic in 1983–84, *J. Phys. Oceanogr.*, *18*, 1855–1875, 1988.

Hernandez, F., P. Y. Le Traon, and R. Morrow, Mapping mesoscale variability of the Azores Current using TOPEX/POSEIDON and ERS-1 altimetry, together with hydrographic and Lagrangian measurements, *J. Geophys. Res.*, *100*, 24,995–25,006, 1995.

Jourdan, D., Etude des conditions hydrologiques dans le bassin Canaries-Acores, technical report, Serv. Hydrogr. et Oceanogr. de la Mar., Toulouse, France, 1994.

Käse, R. H., and W. Krauss, The Gulf Stream, the North Atlantic Current, and the origin of the Azores Current, in *The Warmwatersphere of the North Atlantic Ocean*, edited by W. Krauss, pp. 291–331, Gebrüder Bornträger, Berlin, 1996.

Käse, R. H., and G. Siedler, Meandering of the subtropical front south-east of the Azores, *Nature*, *300*, 245–246, 1982.

Käse, R. H., and W. Zenk, Structure of a Mediterranean water and meddy characteristics in the Northeastern Atlantic, in *The Warmwatersphere of the North Atlantic Ocean*, edited by W. Krauss, pp. 365–393, Gebrüder Bornträger, Berlin, 1996.

Käse, R. H., W. Zenk, T. B. Sanford, and W. Hiller, Currents, fronts and eddy fluxes in the Canary Basin, *Prog. Oceanogr.*, *14*, 231–257, 1985.

Käse, R. H., J. F. Price, P. L. Richardson, and W. Zenk, A quasi-synoptic survey of the thermocline circulation and water mass distribution within the Canary basin, *J. Geophys. Res.*, *91*, 9739–9748, 1986.

Kielmann, J., and R. H. Käse, Numerical modeling of meander and eddy formation in the Azores Current frontal zone, *J. Phys. Oceanogr.*, *17*, 529–541, 1987.

Klein, B., and G. Siedler, On the origin of the Azores Current, *J. Geophys. Res.*, *94*, 6159–6168, 1989.

Krauss, W., R. H. Käse, and H.-H. Hinrichsen, The branching of the Gulf Stream southeast of the Grand Banks, *J. Geophys. Res.*, *95*, 13,089–13,103, 1990.

Le Traon, P. Y., Time scales of mesoscale variability and their relationship with spatial scales in the North Atlantic, *J. Mar. Res.*, *49*, 467–492, 1991.

Le Traon, P. Y., and P. De Mey, The eddy field associated with the Azores Front east of the Mid-Atlantic Ridge as observed by the Geosat altimeter, *J. Geophys. Res.*, *99*, 9907–9923, 1994.

Le Traon, P. Y., and F. Hernandez, Mapping the oceanic mesoscale variability: Validation of satellite altimetry using surface drifters, *J. Atmos. Oceanic Technol.*, *9*, 687–698, 1992.

McCartney, M. S., and L. D. Talley, The Subpolar Mode Water of the North Atlantic Ocean, *J. Phys. Oceanogr.*, *12*, 1169–1188, 1982.

Morrow, R., and P. De Mey, Adjoint assimilation of altimetric, surface drifter, and hydrographic data in a quasi-geostrophic model of the Azores Current, *J. Geophys. Res.*, *100*, 25,007–25,025, 1995.

Müller, T., and G. Siedler, Multi-year current time series in the North Atlantic Ocean, *J. Mar. Res.*, *50*, 63–98, 1992.

Paillet, J., M. Arhan, and M. S. McCartney, Spreading of Labrador Sea Water in the eastern North Atlantic, *J. Geophys. Res.*, *103*, 10,223–10,239, 1998.

Richardson, P. L., and A. Tychensky, Meddy trajectories in the Canary Basin measured during the SEMAPHORE experiment, 1993–1995, *J. Geophys. Res.*, this issue.

Siedler, G., and R. Onken, Eastern recirculation, in *The Warmwatersphere of the North Atlantic Ocean*, edited by W. Krauss, pp. 339–360, Gebrüder Bornträger, Berlin, 1996.

Siedler, G., W. Zenk, and W. J. Emery, Strong current events related to a subtropical front in the northeast Atlantic, *J. Phys. Oceanogr.*, *15*, 885–897, 1985.

Spall, M. A., Circulation in the Canary Basin: A model/data analysis, *J. Geophys. Res.*, *95*, 9611–9628, 1990.

Stramma, L., Geostrophic transport in the Warm Water Sphere of the eastern subtropical North Atlantic, *J. Mar. Res.*, *42*, 537–558, 1984.

Stramma, L., and G. Siedler, Seasonal changes in the North Atlantic subtropical gyre, *J. Geophys. Res.*, *93*, 8111–8118, 1988.

Sy, A., Investigation of large-scale circulation patterns in the central North Atlantic: The North Atlantic Current, the Azores Current, and the Mediterranean Water plume in the area of the Mid-Atlantic Ridge, *Deep Sea Res., Part A*, *35*, 383–413, 1988.

Tychensky, A., and X. Carton, Hydrological and dynamical characterization of Meddies in the Azores region: A paradigm for baroclinic vortex dynamics, *J. Geophys. Res.*, this issue.

F. Hernandez and P.-Y. Le Traon, Collecte Localisation Satellites, 8–10 rue Hermès Parc Technologique du Canal, 31526 Ramonville St.-Agne, France.

D. Jourdan and A. Tychensky, Service Hydrographique et Océanographique de la Marine, Centre Militaire d'Océanographie, 14 avenue Edouard Belin, 31401 Toulouse, Cedex 4, France. (e-mail: Aude.Tychensky@cnes.fr)

(Received February 20, 1997; revised February 9, 1998; accepted March 9, 1998.)